

# A Study of the Influence of Fines and Fibre Length on the Vacuum Filtration of Cellulose Fibres from Recycled Paper Resources



Master's Thesis  
Maria Sigsgaard  
December 2009  
Aalborg University

A Study of the Influence of Fines  
and Fibre Length on the Vacuum  
Filtration of Cellulose Fibres  
from Recycled Paper Resources

**M.Sc. Thesis:** 9<sup>th</sup> and 10<sup>th</sup> semester,  
September 1<sup>st</sup> 2008 -  
December 4<sup>th</sup> 2009

**Participant:**

Maria Sigsgaard

**Supervisor:**

Kristian Keiding

**Danish title:** En undersøgelse af fines  
og fibrelængdens indflydelse på  
vakuumpiltrering  
af cellulose fibre fra genbrugte pa-  
pirressourcer

**Printings:** 5

**Number of Pages:** 66

**Number of Enclosures:** 1 + CD-rom

---

Maria Sigsgaard

**Abstract:**

In this Master's Thesis the length of recycled cellulose fibres from five different sources of paper are examined in order to study its influence on the vacuum filtration of pulps. The understanding of the fibres influence on the dewatering process is necessary to optimize the process. The size distribution are wider in the pulps of newsprint, when compared to the size distribution of printing papers.

Newsprint pulps has a longer filtration time than pulps of printing paper, and a poorer dry-matter content in the filter cakes.

The specific filter cake resistance is calculated from Ruth plots, and is larger in the filter cakes consisting of newsprint than printing paper.

The Kozeny-Carman equation is used in order to find a correlation between surface area of the fibres and flux of filtrate. However, the standard deviations of the fibre sizes are too high to use the Kozeny-Carman relation. Instead, it is concluded that the lower size distribution of fibres in printing papers results in lower filtration time and better dewatering of the filter cakes.

Filter cakes from recycled newsprint appears to have a larger max load and to be a more brittle material than printing paper. When pressure is applied in a three point bending test, there seems to be no difference between the filter cakes from either newsprint or printing paper.

When adding just 10 % (w/w) of another type of pulp to a pulp, the filtration time improves and the drymatter content in the filter cakes increases. A pulp consisting of 30 % (w/w) newsprint and 70 % (w/w) printing paper with a mean size of  $1.08 \pm 0.78$  mm has the best filtration regarding both filtration time and dry-matter content of the cake.



# Dansk resumé

I forbindelse med dette afgangsspeciale er længden af genbrugs cellulose fibre fra fem forskellige ressourcer undersøgt med henblik på at studere dens indflydelse på vakuum afvanding af papir pulpe. Forståelsen af fibrenes indflydelse på afvandingsprocessen er nødvendig for at kunne optimere den.

Størrelsesfordelingen er bredere i pulpene af avispapir end i pulpene bestående af kopipapir.

Pulpe af avispapir har en længere filtreringstid end pulpene af kopipapir og et mindre tørstofindhold i filterkagerne.

Den specifikke filterkagemodstand er beregnet ud fra Ruth plot og er større ved filterkagerne fra avispapir end fra kopipapir.

Kozeny-Carman ligningen er anvendt for at finde en sammenhæng mellem fibrenes overfladeareal og flux-en af filtrat. Standardafvigelserne på fiber størrelserne er for store til at den kan anvendes. Istedet er det konkluderet, at den lavere størrelsesfordeling resulterer i en lavere filtreringstid og bedre afvanding af filterkagerne.

Filterkager fra avispapir virker til at kunne tåle et større træk og er mere skrøbelig end filterkager fra kopipapir. Der virker ikke til at være forskel på filterkagerne når trykket tilføres i en tre-punkts styrketest.

Ved tilsætning af kun 10 % pulp til en anden pulp, nedsættes filtreringstiden og tørstofindholdet i filterkagerne øges. En pulp bestående af 30 % (w/w) avispapir og 70 % (w/w) kopipapir med en gennemsnitstørrelse på  $1.08 \pm 0.78$  mm har den bedste afvanding når man ser på afvandingstid og tørstofindhold af filterkagen.



# Preface

The Chinese invented paper in the second century. It took over 600 years before it reached Europe and today the process of making paper is still not fully understood.

Especially in these days of environmental concern the recycling is in focus in order to obtain a better image.

Producing new products from recycled paper is an advantage in the competition, as the amount of paper used worldwide is still growing. With the larger amount of used paper a larger amount of that is recycled.

This Master's Thesis is completed at Aalborg University as a final part of the education for Master of Science in Engineering, Chemistry.

References are stated in square brackets [Author, year] and can be found in the Bibliography.

A list of Nomenclature is placed before the Bibliography.

The figures, tables and equations are consecutive numbered throughout the chapters. The enclosed CD contains excel sheets with data, the few articles available as PDF, a appendix full of Ruth plots and an electronic version of the Masters' Thesis.

## Acknowledgment

I would like to acknowledge the following persons:

Project manager Rasmus Friche, from Brødrene Hartmann A/S for support and input throughout the entire project.

Morten Møller Klausen, from DHI for lending me his filtration apparatus and his results from own experiments.

Lisbeth Wybrandt, laboratory technician AAU, for performing AAS-experiments.

Henrik Koch and Kim Mørkholt, Assistant Engineers AAU, for helping out when my practical skills were too low.

Mikkel Agerbæk, Flemming Thorsen and Jakob Vang Jensen from Teknologisk Institut Århus, for help with performing the strength and bending tests.

Anette Lindé and Margaretha Fryklund from Innventia AB for measuring the size distributions of fibres.

Anders Duelund and Tea Rasmussen for help with stress and strain theory.

Ludmilla Lumholdt Riisager for linguistic corrections.

Mads Koustrup Jørgensen for help with detection of excel errors.

The following persons for answering my questions on the paper sources:

- Lars Lundberg and Tine Hansen from Xerox Denmark.
- Bo Morsing from Multicopy Denmark.
- Kim Holten Larsen from MetroXpress.
- Peter Hagdrup from Urban.
- Søren Winlsøw from Pressens Fællesindkøb.



# Contents

<b>1</b>	<b>Introduction</b>	<b>1</b>
1.1	Thesis statement . . . . .	2
1.2	Plan for thesis . . . . .	2
<b>2</b>	<b>Theory</b>	<b>4</b>
2.1	From tree to paper . . . . .	4
2.2	Vacuumfiltration . . . . .	8
2.3	Characterization of filter cakes . . . . .	12
<b>3</b>	<b>Experimental approach</b>	<b>15</b>
3.1	Presentation of paperressources . . . . .	15
3.2	Demands for cake filtration . . . . .	15
3.3	Allow for heterogenity . . . . .	16
<b>4</b>	<b>Experimental</b>	<b>18</b>
4.1	Characterization of paper ressources . . . . .	18
4.2	Pulping . . . . .	18
4.3	Filtration . . . . .	18
4.4	Characterization of filtrate . . . . .	20
4.5	Strength analysis of filter cakes . . . . .	20
<b>5</b>	<b>Results</b>	<b>22</b>
5.1	Fibre ressources . . . . .	22
5.2	Filtrations on the paper ressources . . . . .	27
5.3	Concentration of $\text{Ca}^{++}$ in pulp and filtrate . . . . .	33
5.4	Strength analysis . . . . .	33
5.5	Variation experiment . . . . .	39
<b>6</b>	<b>Discussion</b>	<b>43</b>
<b>7</b>	<b>Conclusion</b>	<b>48</b>
<b>8</b>	<b>Nomenclature</b>	<b>49</b>
	<b>Bibliography</b>	<b>51</b>
<b>A</b>	<b>Hartmann Process</b>	<b>54</b>



# 1. Introduction

Since most sorts of papers, e.g. newsprint, writing and printing paper etc., are recycled, the paper industry can use this as a source of fibre. Cellulose fibres from e.g. trees are called virgin fibers, while fibers from already processed paper is called recycled fibers [Göttsching and Pakarinen, 2000]. The recycled fibers can be used as supplement to the virgin fibers or alone in new products [Göttsching and Pakarinen, 2000]. Recycled fibers and virgin fibers reacts diverse when treated the same [Göttsching and Pakarinen, 2000]. Water removal of the pulp of fibres in paper industry is one of the processes demanding most energy [Ramaswamy, 2003]. An understanding of the mechanism of water removal from pulp slurries is necessary in order to characterize the entire process [Ingmanson, 1952]. Vacuum filtration is used widely in the paper industry as a dewatering process. Vacuum filtration at the stage of air breakthrough is characterized by the largest pores being drained for water, and air flow through the filter cake is present. Meanwhile the smaller pores can still hold water [Condie et al., 1996].

Many models of the dewatering process exists in order to take regard to the various factors such as temperature, dwell time, flocculating agents, etc., which influences the dewatering [Ramaswamy, 2003]. These models describe the dewatering in the branch of the the paper industry producing their products on a wire. Here, the dewatering process takes place when the flat mat of pulp is passing over a suction box with vacuum [Walker, 2006].

Brødrene Hartmann A/S produces moulded fibre products from recycled newsprint and paper advertises. The dewatering process is performed when a form of metal mesh is submerged into a chest of pulp slurry using the vacuum to form the product and later when not longer submerged, to remove the water. The process is further described in appendix A on page 54. This make the models, described in the summary by Ramaswamy (2003), inapplicable, since they are not fully comparable with the process at Brødrene Hartmann A/S. A model of the dewatering process has to be redeveloped in order to describe the Hartmann process.

Different stages in the process of Brødrene Hartmann A/S has been examined to understand their influence on the dewatering process. Experiments have shown, that the specific filter cake resistance increases with increased bacterial growth, and the bacteria present in the process influences directly on the dewatering by effecting the charge condition and surface condition in the pulp slurry [Lundgaard and Nielsen, 2005]. The short duration of dewatering implies that creep has no effect on the dewatering process. Therefore the strategy of flocculating can be developed regardless to creep [Stougaard and Jensen, 2006]. Application of flocculating agents enhances the dewatering [Roberts, 1996]. The flocculation strategy has changed over the years in order to improve the dewatering or to fulfill the legislations.

Regarding the interdisciplinary collaboration between various science institutes and companies named PAKK (Productions optimization in Applied Colloidal Chemistry). Brødrene Hartmann A/S was one of these companies and experiments conducted by DHI revealed that both pulping time and mass of dried filter cake influences on the filtration time.

When the process at the plants of Brødrene Hartmann A/S is characterized an optimization of it can begin. To obtain the most effective optimization, all the variables has to be known, both the ones from the machinery and the ones from the dewatering process [Condie et al., 1996]. The length of the fibres influences on the time of dewatering, so the longer the fibre the shorter the dewatering time [Lindau, 2008].

Properties of filtration depends on the packing behavior of the particles [Chellappah et al., 2009]. The packing behavior depends on the distribution of particles' size and shapes. Chellappah et. al (2009) found when mixing fibres with rutile, the settling rate increased and filter cake resistance decreased when just a small amount of fibres were added to the rutile-solution.

The filtrations of particle systems depends on the packing behavior of the particles. A wider distribution of sizes give lower porosity, higher complexity and reduces the effectivity of the filtrations [Chellappah et al., 2009, Dias et al., 2004].

Fibres from different trees and from different pulping processes are not similar and reacts therefore different from one another [Walker, 2006]. Therefore, it is necessary to examine the influence of various fibres on the dewatering process before a complete comprehension of the dewatering process at Brødrene Hartmann A/S can be conducted.

## 1.1 Thesis statement

Is there a difference on the filtration of pulps of different sizes of fibres, and is there a composition of fibres that will retain a minimum of water?

## 1.2 Plan for thesis

In order to fulfill this thesis statement, the following subjects will be examined:

Examine various sources of paper in order to find fibres at different lengths or paper sources with different distribution of fines and fibres.

Perform innumerable vacuum filtrations, measuring time and dewatering of the different pulps.

Examination of the mixing of different pulps.

Characterization of the filter cakes, to investigate, if the different pulps result in lower

strength of the filter cakes.

# 2. Theory

## 2.1 From tree to paper

### 2.1.1 Components in trees

In the paper industry a tree is regarded to consist of three parts: Crown, stem and root system [Karlsson, 2006]. The syem is made up of different parts such as bark, sapwood while the core is called heartwood [Karlsson, 2006].

Trees can have their main period of growth in the spring and is then called earlywood, or in the summer, latewood. In annual rings the earlywood is the light area and the latewood is the dark area. The fast growth in the spring entails large amounts of water being transported up to the new leaves. This means, that the fibres are having large diameter and thin fibre walls when compared to the fibres later produced [Karlsson, 2006].

Trees can be divided into two large groups: softwood and hardwood [Walker, 2006]. Softwood are mostly evergreen, while hardwood are deciduous.

While softwood have long and strong fibres, the hardwood fibres are shorter and thinner. This entails that hardwood fibres gives the paper a smooth surface and high opacity, but the strongest paper is manufactured from softwood [Karlsson, 2006].

Often, printing paper is produced from a mix of hardwood and softwood in order to fulfill the demands for both smooth surface, strength and brightness [Karlsson, 2006].

### 2.1.2 Composition of cell walls of wood fibres

The cell walls consist mainly of cellulose, hemicellulose and lignin [Karlsson, 2006]. Cellulose is a polysaccharide consisting of  $\beta(1-4)$  linked D-glucan, which forms a linear molecule. Hemicellulose is also a polysaccharide but its composition varies according to which source it is from. Lignin is a polymer formed by polymerization from one or more of the following components: *p*-coumaryl, coniferyl and sinapyl alcohols [Evert, 2006].

Two or more strings of cellulose can form a lattice with hydrogen-bondings to one another, called micelles. Micelles and single strain cellulose are part of a microfibril, in which the micelles are kept in place by non-cellulosic materials, like hemicellulose and lignin. The noncellulosic material are black in figure 2.1C. The microfibrils are part of a macrofibril and is kept in place by more non-cellulosic material, black in figure 2.1B. The macrofibril is part of the cell wall [Evert, 2006]. The fibre cell is build up by a lumen (L), primary layer (P), secondary layer consisting of three layers (S1-S3) and middle lamella (M) as

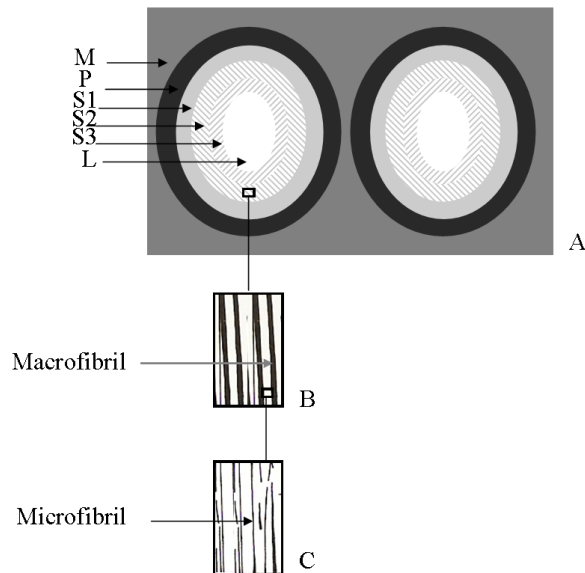


Figure 2.1: Illustration of fibre wall structure and composition thereof. Inspired by [Evert, 2006, Karlsson, 2006]

illustrated in figure 2.1A [Karlsson, 2006]. The middle lamella consist mainly of lignin and is the area between the fibres [Karlsson, 2006]. The distribution of cellulose, hemicelulose and lignin are different from each layer as shown in table 2.1.

Table 2.1: Chemical composition of various layers in the fibre [Karlsson, 2006].

Wall layer	Cellulose [%]	Hemicellulose [%]	Lignin [%]
Middle lamella	0	10	90
Primary wall	10	20	70
Secondary wall, S1	35	25	40
Secondary wall, S2	55	30	15
Secondary wall, S3	55	35	10

Of course there are several other components e.g. pectins and resin [Evert, 2006, Karlsson, 2006].

### 2.1.3 Pulping processes

The process where wood is converted into fibres is called pulping [Karlsson, 2006]. Depending on what kind of tree is used and which product is wanted, there are different kinds of pulping processes which is more beneficial.

#### Mechanical pulping

Mechanical pulping is pulping in which mechanical energy is used to separate the fibres. In this process a high proportion of fibre fragments called fines are produced. Fines are

important in the papermaking process first, because they support the bonding between fibres and second, they prevent opacity by covering the holes in the fibre-web on the papermachine [Walker, 2006]. Fibres from mechanical pulping are chemically unaltered and contain lignin. This makes the fibres stiff and it is also the lignin which make the paper yellow with time when exposed to light [Walker, 2006].

One form of mechanical pulp is Stone Groundwood pulp (SGW). This is produced from debarked billets of wood pressed against a rotating rough stone releasing the fibres and creating fines, approximately 50 % (w/w) of the pulp [Walker, 2006]. Water is added throughout the pulping in order to keep the grinder from overheating.

The SGW process can be altered by adding steam to the grinder, which is called PGW, pressurized groundwood pulping [Karlsson, 2006].

Another method uses wood chips or sawdust instead of billets. This is called Refiner Mechanical pulping (RMP). Between rotating metal discs there is a small opening which is the entrance point for the wood chips. The process can take place under atmospheric pressure or under increased steam pressure. The refiner method generally produces a longer fibre than SGW and lesser fines [Karlsson, 2006].

Thermomechanical pulping (TMP) is a modification of RMP where the wood chips are steamed before and during defibrillation. The steaming gives rise to a softer chip and this results in longer fibres and less fines than RMP and a stronger pulp than both SGW and RMP [Karlsson, 2006].

TMP can be altered, after presteaming a new step is implemented. The chips are submerged into a  $\text{Na}_2\text{SO}_3$ -solution before refining. With this extra step the pulp is called chemithermomechanical pulping (CTMP) [Walker, 2006]. CTMP is often used when producing newsprint [Walker, 2006].

## **Chemical pulping**

The main purpose of making chemical pulps, instead of mechanical pulps, is the removal of lignin [Walker, 2006]. In chemical pulping, the wood chips are pretreated in a chemical solution. This new step is called cooking [Karlsson, 2006]. Adding chemicals and raising the temperature breaks down the lignin to water-soluble parts, which improves the bleaching properties of the chemical pulps, compared with the mechanical pulps [Walker, 2006]. The two main procedures are the alkaline kraft process and acidic sulphite process [Karlsson, 2006].

Kraft pulping is also called sulphate pulping. The cooking liquor is called white liquor and is a blend of sodium hydroxide and sodium sulphite [Walker, 2006]. Kraft pulping is the predominant method used in chemical pulping. This is caused by the high recovery system of the white liquor and the fact that it can be used on all wood species without removing the bark [Walker, 2006].

In the sulphite process the sulphite liquor for the cooking-procedure involves a mixture of

sulphur dioxide, bisulphate ions and sulphite ions. The composition of the sulphite liquor influences the pH-value, e.g. at high pH the liquors consist mainly of sulphite ions while at low pH the liquor is an even mixture of sulphurous acid and bisulphite ions [Walker, 2006]. When the liquor in the sulphite process consists of magnesium bisulphite, the pulp is called magnefite pulp. In table 2.2 the mechanical and chemical pulping processes are compared.

Table 2.2: Comparison of mechanical and chemical pulping

Type of pulping	Mechanical	Chemical
Woodtypes	Softwood and some light hardwood	Softwood and hardwood
Yield	High 90-95 %	Low 40-55 %
Paper strength	Weak	Strong
Bleaching	Diffucult	Easy
Printing Quality	Good	Poor
Description	Fines produced	Pure fibres

### Recycled pulp as a ressource

When the cellulosic ressource is recycled paper of different grades, the process changes [Karlsson, 2006]. The material has to be sorted and cleaned. Stickies, ink and so on have to be removed. Then it is pulped. The ink removal takes place in two step, loosening the ink and separation of the ink from the process water. This is called DIP, Deinked Pulp from recycled fibres RCF [Karlsson, 2006].

#### 2.1.4 Paper Production

When the pulp is made it can be used on the paperwire. The simplest description of the paper wire is that the pulp is spread out on a wire, pressed, dewatered by either vacuum or steam and vacuum, dried and then pressed some more before the formed paper is rolled up on large rollers if it is newspaper or sliced into the wanted sizes [Walker, 2006].

#### 2.1.5 Recycled paper

A larger amount of paper is every year recycled either to be burned and to make heat or to create new products [Ingmanson, 1952]. Recycled fibres can be reused 5-6 times [Karlsson, 2006]. There is a differece between the new fibres, called virgin fibres and the recycled fibres [Ingmanson, 1952]. Recycled fibres are more stiff.

## 2.2 Vacuumfiltration

The laws of filtration is a concept used to describe the main mechanisms of filtration [Wakeman and Tarleton, 1999]. The standard blocking filtration is when the particle size is smaller than the pore sizes and the particles are captured predominantly inside the filter medium.

Complete blocking filtration is when the particle is larger than the pore size and the particles are captured by blocking the pores. This means that the filtermediums surface is unusable for further filtrations.

Bridging filtration is when the particles are smaller than the pores, but the particles are captured on the surface of the filtermedium since the particles form stable and permeable bridging.

Intermediate blocking filtration is when the particles are larger than the pores, but not necessarily will block the pores when captured. This leaves the possibility that particles, which will arrive later, can rest on already deposited cakes. Again, bridging can occur.

### 2.2.1 Filtration of filter cake

During dewatering in dead-end filtrations the height of the filtercake increases with time. The process can be divided into three stages: Initial, accumulation and consolidation. The initial stage is before and during initial cakeformation, accumulation stage is when the formed cake increases in thickness while consolidation stage is when the piston touches the cake and presses the final water out.

In vacuum filtration the initial and accumulation stages are similar but the consolidation stage differ. Instead of a piston, the vacuum sucks the air over the filter cake down through the waterfilled pores. This means that with breakthrough of air the vacuum ceases and the filtration is done [Condie et al., 1996]. The formation of filter cake during vacuum is illustrated in figure 2.2.

Figure 2.2A shows the vacuumfiltration before start. Figure 2.2B illustrates the cakeformation, before a sufficient amount of fibres are maintained by the filter to form a fibre-web.

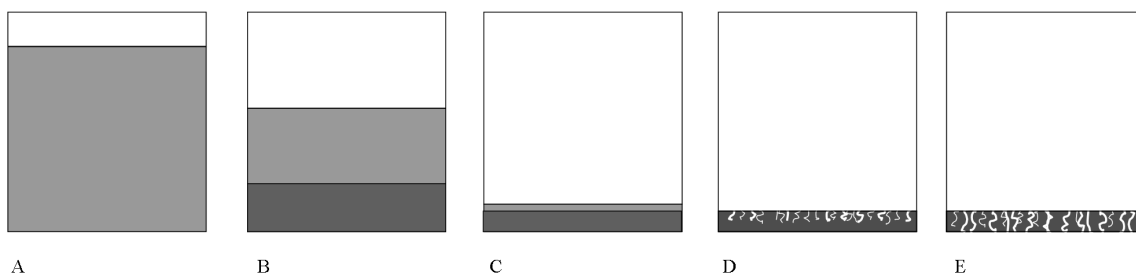


Figure 2.2: Illustration of the principles in vacuum filtration. Inspired by [Condie et al., 1996].

All the fines, both primary and secondary, end in the filtrate. When a sufficient amount of cake is formed the fines are retained in the fibre-web, which a filter cake consists of. Just before the surface of the remaining pulp touches the surface of the cake, the cake is almost as high as possible. When no pulp is above the surface of the cake, as illustrated in 2.2D, the cake consolidates and allows air to start filling up the pores in the filtercake. When breakthrough of air, the filtration is over, as illustrated in 2.2E. The larger the pores, the faster the dewatering. This means, that the improvement of the dewatering by using only large fibres is minimized by the large gaps in paper and loss in strength of final product.

The filtration is effected by the particle size, distribution of fibres, shape of particles and surface properties [Wakeman and Tarleton, 1999].

### 2.2.2 Derivation of Darcy's law

According to Darcy one could describe a filtration process from a simple equation 2.1, also called Darcy's law, [Wakeman and Tarleton, 1999]:

$$u = \frac{-k dP}{\mu dz} \quad (2.1)$$

Where  $u$  is the volume flow rate pr. unit cross-sectional area of the bed,  $k$  is the permeability,  $\mu$  is the viscosity and  $dP$  is the difference in hydraulic pressure across the thickness of filter medium  $dz$ .

$u$  can also be written  $\frac{dV}{A*dt}$ , where  $dV$  is the change in volume during the period of time,  $dt$ , and  $A$  is the cross-sectional area. Inserting this and rearranging equation 2.1:

$$\frac{dV}{dt} = \frac{AkdP}{dz} \quad (2.2)$$

Utilizing the factors connected to the filtermedium  $k$  and  $dz$ , the filter medium resistance  $R_m$  is equal to  $\frac{dz}{k}$ , equation 2.2 can be rewritten [Tao et al., 2003]:

$$\frac{dV}{dt} = \frac{AdP}{\mu R_m} \quad (2.3)$$

When a cake is build up during the filtration, also called cake-filtration, the filtermedium resistance alone can not be used to describe the full resistance, therefore a new part called the cake resistance,  $R_c$  is necessary [Tao et al., 2003].

$$\frac{dV}{dt} = \frac{AdP}{\mu(R_m + R_c)} \quad (2.4)$$

$R_c$  can be assumed to be directly proportional to the amount of cake deposited  $w$ , with the specific filtercake resistance  $\alpha$ , as the proportionality factor, i.e.:  $R_c = \alpha w$ . This means

that equation 2.4 on the preceding page can be written:

$$\frac{dV}{dt} = \frac{AdP}{\mu(R_m + \alpha w)} \quad (2.5)$$

$w$  is related to the volume of filtrate,  $V$ , by:  $wA = sV$ , where  $s$  is the concentration of solid in slurry. This implemented to equation 2.5 gives:

$$\frac{dV}{dt} = \frac{A^2dP}{\mu(R_mA + \alpha sV)} \quad (2.6)$$

Rearranging equation 2.6:

$$\frac{dt}{dV} = \frac{\mu R_m}{AdP} + \alpha \frac{\mu s}{A^2dP} V \quad (2.7)$$

Integration of equation 2.7 has the following solution under the assumption that  $dP$  is constant:

$$\int_0^t dt = \int_0^V \frac{\alpha \mu s}{A^2 dP} V dV + \int_0^V \frac{\mu R_m}{AdP} dV \quad (2.8)$$

⇕

$$t = \frac{\alpha \mu s}{A^2 dP} \left[ \frac{1}{2} V^2 \right]_0^V + \frac{\mu R_m}{AdP} [V]_0^V \quad (2.9)$$

⇕

$$t = \frac{\alpha \mu s}{2A^2 dP} V^2 + \frac{\mu R_m}{AdP} V \quad (2.10)$$

Equation 2.10 can be rearranged into:

$$\frac{t}{V} = \frac{\alpha \mu s}{2A^2 dP} V + \frac{\mu R_m}{AdP} \quad (2.11)$$

From equation 2.11 the plotting of  $\frac{t}{V}$  versus  $V$  indicates that from the slope and intercept it would be possible to calculate  $\alpha$  and  $R_m$ , respectively, if the pressure is constant. It is also possible to calculate these from equation 2.7, when plotting  $\frac{dt}{dV}$  against  $\frac{V}{dP}$ , here the pressure can vary.

Calculating  $\alpha$  and  $R_m$  from experiments performed under different conditions or by varying a single factor the effect on the filtercake and filtermedium can be evaluated [Tao et al., 2003].

As derived above, Ruth Plot only applies for the incompressible filtercakes. Filtercakes of paperfibre are compressible, but during vacuum filtration the pressure is applied from below and therefore no pressure are on top of the cake to compress it and therefore it is possible to use Darcy's law concerning incompressible filtercakes [Condie et al., 1996].

### 2.2.3 Derivation of Kozeny-Carman equation

In filtration of filter cakes consisting of cellulose fibres, a laminar flow occurs and therefore the Poisselle equation can be used to describe the dewatering of the filter cakes [Wakeman and Tarleton, 1999].

$$\frac{\Delta P}{h} = k_1 \frac{v\mu}{D_h^2} \quad (2.12)$$

When the pores are not circular the hydraulic diameter  $D_h$ , is used to characterize the pores,  $\Delta P$  is the difference in pressure,  $h$  is the height of the cake.  $k_1$  is a constant, since the height of the cake is lower than the pore length, because of the tortoisity. The porosity of the cake,  $\phi$ , can be described by [Clement et al., 2004]:

$$\phi = \frac{V_{pores}}{V_{tot}} \quad (2.13)$$

As porous structures result in longer pores, the velocity is connected to  $\phi$ :

$$v_0 = v\phi \quad (2.14)$$

Isolating  $v = \frac{v_0}{\phi}$  and inserting in equation 2.12:

$$\frac{\Delta P}{h} = k_1 \frac{v_0\mu}{\epsilon \cdot D_h^2} \quad (2.15)$$

$D_h$  is hydraulic diameter of pores [Clement et al., 2004]:

$$D_h = \frac{k_2 \cdot V_{pore}}{k_3 A_{pore,surface}} \quad (2.16)$$

As  $V_{pore} = A \cdot h\phi$  and  $A_{pore,surface} = S_o Ah(1-\phi)$ . where  $S_o$  is the area of particles divided by the volume of particles [Wakeman and Tarleton, 1999].

$$D_h = k_4 \frac{A \cdot l \cdot \phi}{S_o \cdot A \cdot h(1-\phi)} \quad (2.17)$$

when inserting equation 2.17 in equation 2.15:

$$\frac{\Delta P}{h} = k_1 \frac{v_0\mu}{\phi \cdot \left( \frac{k_4 \cdot h \cdot \phi}{S_o \cdot h \cdot (1-\phi)} \right)^2} \quad (2.18)$$

$$\frac{pf}{l} = k_1 \frac{v_0\mu}{\frac{k_4^2 \cdot h^2 \cdot \phi^3}{S_o^2 \cdot h^2 \cdot (1-\phi)^2}} \quad (2.19)$$

$$\frac{\Delta P}{h} = k_5 \frac{v_0\mu * (1-\phi)^2}{\phi^3} * S_o^2 \quad (2.20)$$

where  $k_5 = k_1/k_4^2$ , and  $S_o$  is the specific surface of a cylinder, since this is the simplest way to describe a fibre.

$$S_o = \frac{2\pi \cdot r \cdot l_{fibre} + 2\pi \cdot r^2}{l - fibre\pi r^2} = \frac{2}{r} + \frac{2}{h} \quad (2.21)$$

Where  $l - fibre$  is the length of the fibre and  $r$  is the radius in the cross sectional area of the fibre. Equation 2.20 can be rewritten to:

$$v_0 = \frac{\phi^3 h}{\Delta P k_5 \mu (1 - \phi)^2 S_o^2} \quad (2.22)$$

From equation 2.22 the influence of the specific surface of fibre on the dewatering can be described.

## 2.3 Characterization of filter cakes

### 2.3.1 Tensile stress test

A way to characterize the filter cakes is to perform a tensile test on them. This can reveal the mechanical properties of the materials. The tensile test makes it possible to measure the strains and calculate the stresses of the material [Norton, 2006].

The stresses,  $\sigma$ , is defined as load pr. unit area:

$$\sigma = \frac{P_{load}}{A_0} \quad (2.23)$$

Where  $P_{load}$  is the applied load and  $A_0$  is the initial cross sectional area.

Strain,  $\epsilon$ , is the change in length pr. unit length and can be calculated from:

$$\epsilon = \frac{l - l_0}{l_0} \quad (2.24)$$

Where  $l_0$  is the original length of the unit and  $l$  is the length at any load,  $P_{load}$ . Plotting  $\epsilon$  against  $\sigma$  gives the association of the forces in the specimen tested, called a tensile test [Norton, 2006].

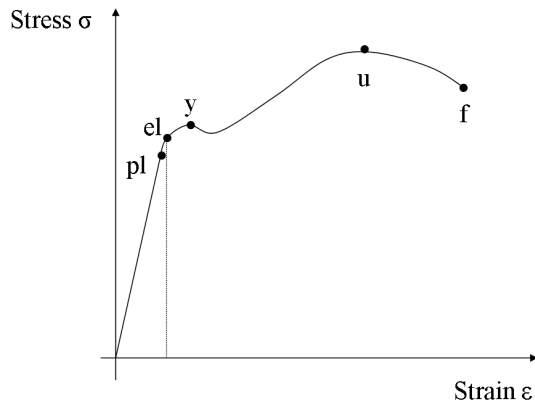


Figure 2.3: A stress-strain diagram of a ductile material. Inspired by [Norton, 2006]

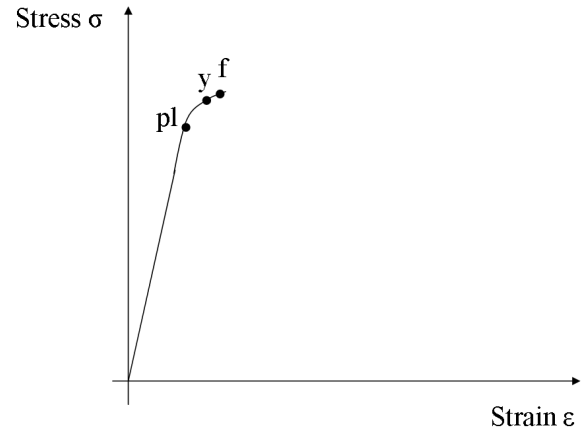


Figure 2.4: A stress-strain diagram of a brittle material. Inspired by [Norton, 2006]

The material can either be ductile or brittle. The stress-strain diagram will show if the material is one or the other, since the behavior of them is not the same. When a ductile material is exposed to the tensile stress test, the stress-strain diagram will look like figure 2.3. If the material is brittle, without a negligible plastic range, and is exposed to the tensile stress test, the curve would more look like the stress-strain diagram in figure 2.4. Both ductile and brittle materials have an elastic region, where the strain and stress are proportional until the proportional limit,  $P_l$  is reached. The correlation is valid when the samples are stretched in one dimension and samples are isotropic and linearly elastic as illustrated in figure 2.5.



Figure 2.5: Schematic overview of the experimental set up of the tensile stress test.

The correlation between  $\sigma$  and  $\epsilon$  is called Hooke's law [Norton, 2006]:

$$E = \frac{\sigma}{\epsilon} \quad (2.25)$$

where  $E$  is the slope of the strain-stress diagrams elastic region also called the Young's Modulus or the modulus of elasticity. Young's modulus is a measure of the materials stiffness and has the unit of the stresses.

The elastic limit,  $e_l$  defines the point where permanent deformations of the material starts to occur. In other words, it is the point between plastic range and elastic range [Norton, 2006].

The point  $y$ , symbolizes the yield strength. It occurs, when the rate of deformation increases as seen by a lower slope. The stress value apperting to yield strength is called

$S_y$ .

$S_u$  is the ultimate tensile strength, which is the maximum stress, the material can handle before breaking. Sometimes the material has a reduction in area when it is ductile. This is seen by the necking down between  $u$  and  $f$ .

The specific strength of a material is defined as the strength divided by the density, since the stress is only based on  $A_0$ . This is also called the strength to weight ratio (SWR)[Norton, 2006].

The specific stiffness is Young's Modulus divided by sample density.

When the calculations are done without taking into consideration, that the cross sectional area is changing during the test, it is called engineering stress-strain curve.

### 2.3.2 Bending test

The tensile stress machine can run in reverse, so instead of pulling the sample apart, a bending test can be performed.

When the bending test is performed as a three-point strength test, the sample is simply supported in each end and pressed down in a point between. As illustrated by figure 2.6.

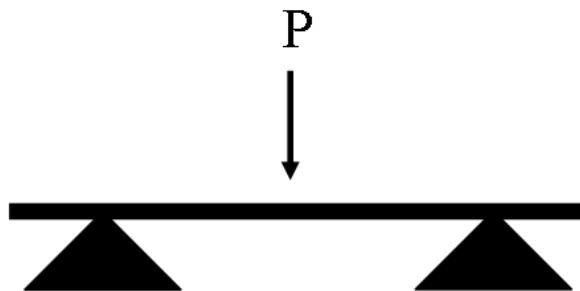


Figure 2.6: Schematic overview of a three-point bending test.

A stress-strain diagram analogue to the one of the tensile stress test can not normally be drawn because the the stress distribution over the cross sectional area varies. The bending stresses are tensile on the convex side of the material and compressive on the concave side. The stresses in bending test is used to predict failure in bending, where the stresses of the tensile stress test is used to predict, if the material is brittle or ductile [Norton, 2006]. The strain affecting tensile stress is positive, while the strain affecting compressive stresses are negative.

Normally it is impossible to apply stress and strain to deformations experiments since the pressure is applied at one point instead of over the whole sample [Norton, 2006]. But when the pressure is applied to the sample in the width of the cross sectional area instead of in one point, it should be possible.

## 3. Experimental approach

In order to compare the different resources it is important to treat them similarly, so the difference measured is the actual difference between the resources.

### 3.1 Presentation of paperresources

Five different sources of paper sources were selected. Two different types of newsprint and three different kind of printing paper. The newspapers were Urban (A1) and MetroXpress (A2). The printing paper were Xerox Business (B1), Xerox Premiere (B2) and Multicopy (B3).

MetroXpress is printed on 42 g/m<sup>2</sup> paper produced by Holmen, Sweden. It is produced from spruce xylem or recycled paper. They produce paper from either TMP or DIP (See 2.1.3 on page 7).

Urban is being printed at Trykkompagniet, who use 42.4 g/m<sup>2</sup> paper from either Norske Skog or Stora Enso. Both papermills uses spruce and recycled paper. Both uses mechanical pulping to release the cellulose.

Both Xerox Business and Xerox Premiere is produced with chemical pulping and bleached afterwards. They are uncoated and produced without any recycled fibres. It is produced from various trees both hardwood and softwood. Xerox Premiere is 90 g/m<sup>2</sup> and Xerox Business is 80 g/m<sup>2</sup>.

Multicopy is produced by Stora Enso from Roundwood (Spruce, Pine, Beech, Eucalyptus and Aspen) and sawmill chips. They use magnefite pulping as pulping method, using magnesium bisulphite as the liquor. It contains 80 g/m<sup>2</sup>.

The above mentioned implies that the main difference in the paper sources is the pulping method. Both newspapers can contain recycled fibers which can influence the pulps more in the experiments.

### 3.2 Demands for cake filtration

To obtain a usable product from cake filtration there are some demands which have to be fulfilled.

First the fibres in the pulp have to be separated totally to create a good cake.

In order to make a formstable product, the dewatering has to be good and uniform. Large fibres create a cake with low opacity and therefore not a stable product. Small fibres create a cake with high opacity, but the dewatering of this is time demanding. Therefore a mix

of fibre lengths will be favorable in order to opacity, form stability and dewatering time. In order to get as much water out by vacuum filtration the pores in the cake have to be uniform, because when there is a breakthrough of air the dewatering is minimal. Various factors beside the fibres can effect the dewatering: Sedimentation, cludging of pores, creep, consolidation and heterogenous cake. These will effect the dewatering in a negative way with a lower rate of dewatering.

### **3.3 Allow for heterogeneity**

When working with something as heterogenous as paper pulp, the best way to reduce the influence of heterogeneity is to measure on large sample amounts. When this is not possible, repetition is the best way to avoid uncertainties in the results. Therefore double or triple determination can help by validating the results.

The determination of drymatter content in the paper source is important, since it is this calculation, which determines the water-paper composition in the pulp.

According to Wakeman and Tarleton (1999) the zeta potential can effect the particles. Especially zeta potentials around the iso-electrical point, will entail influence on filtration e.g. the dewatering rate and the drymatter content in the filter cakes. Furthermore the fibres will possible aggregate since the net repulsive forces are small.

The trouble areas of the experiments consist of the pulping, the filter cakes and the filtrate.

#### **3.3.1 Pulping**

According to experiments the pulping time effects the dewatering time, so in order to compare the different pulps with others of same kind and with the other types of pulp, the pulping time has to be constant.

The characterization of fibres in different pulps is important, as the size distribution and zetapotential define the fibres and thereby the various pulps.

#### **3.3.2 Filter cakes**

The filtrations where conducted in order to obtain a final drymatter content in the filter cakes of 400 g/m<sup>2</sup>.  $\alpha$  is a constant which reveals the specific filter cake resistance in the filtration and with low standard deviations the tendencies of the various pulps. Strain Stress test can help to understand the dry filter cakes and describe the stiffness of material by finding the Young's Modulus for the filter cakes.

### 3.3.3 Filtrate

To see if there is a difference in the retention of fines of the various pulps and in one type of pulp the drymatter content in filtrate is measured. The determination of the concentration of  $\text{Ca}^{++}$  in both the pulp and filtrate can reveal the retention by filtercakes.

# 4. Experimental

## 4.1 Characterization of paper resources

### 4.1.1 Measuring fibre sizes

3 % (w/w) samples of the different fibre resources were diluted to 10 mg/L and sent to Innventia A/S, Sweden for further analysis on L&W Fiber Tester, ISO 5263-1:2004. The fibres were analyzed at 40-45 °C.

### 4.1.2 Zetapotentiale

Approximately 0.1 g of 3 % (w/w) pulp of each sample was dissolved into 100 ml of tap water. The Zetamaster (Malvern Instruments Inc.) was reset with Min-U-sil, the cell was flushed with 40 mL of demineralized water and then approximately 10 mL of sample was injected into the Zetamaster. The cell was flushed with 40 ml of demineralized water between each sample. It measured 5 times on each sample and 2 samples of each pulp was analysed.

### 4.1.3 Drymatter content and ash content

Three pieces of paper were placed in three pre-weighed foil forms and weighed. Then they were placed at 105 °C in at least 24 hours before weighed again. After the weighing, the forms were placed in a muffle oven at 560 °C for at least 12 hours and then weighed again.

## 4.2 Pulping

The paper source was added along with water to a drymatter content of 3 % (w/w). The foodprocessor (BRAUN 3210, Germany) was started at highest level and blended for 5 min. After scraping the pulp of the lid and sides, the foodprocessor was started again for 10 minutes. After scraping the residues the foodprocessor was started for 15 min.

## 4.3 Filtration

Before filtration, the pulp was diluted to a drymatter content on 1 % (w/w) with demineralized water. Approximately 154 g of pulp was weighed into a container so the final

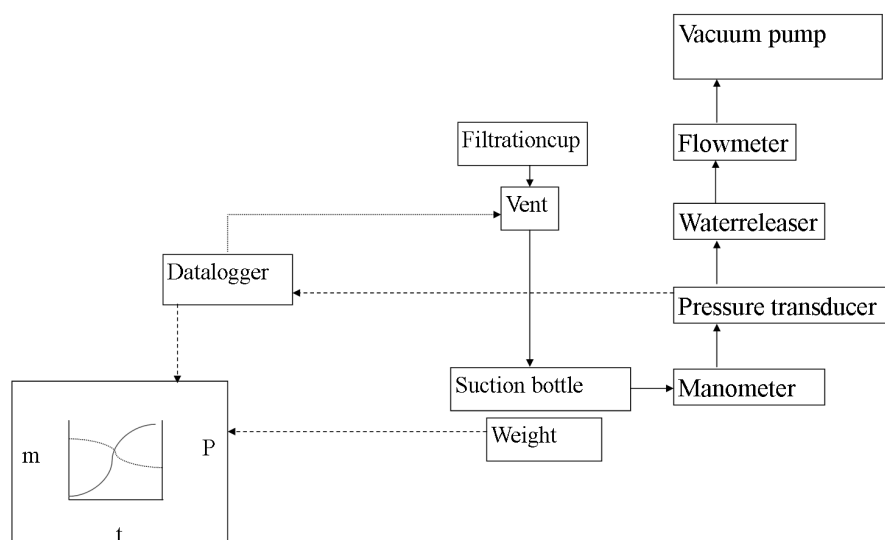


Figure 4.1: Flowdiagram of set up for filtration

filtercake would contain  $400 \text{ g/m}^2$  fiber. Figure 4.1 shows the set up of the filtration apparatus. The filtration apparatus was connected, then the pump was turned on, vacuum was built up, the pulp was twirled around in the container before poured into the filtration cup, inner diameter 7 cm. When the manometer stabilized around 0.5 bar of vacuum the filtration was started. During filtration the pressure and weight was logged 5 times each second.

### 4.3.1 Filtrations on mixed pulps

Additional filtrations were carried out on pulps consisting of both paper ressource A1 and B1 in different ratios. The amount of pulp weighed were still 154 g, and the composition of the pulp were 90:10, 70:30, 50:50, 30:70 and 10:90 % (w/w) of A1 and B1, respectively. After filtration, the drymatter content of the filter cakes and filtrate were measured.

### 4.3.2 Filtration to strength analysis

For the strength analysis of the filter cakes a different filtration setup was used in order to enlarge the testing material. Approximately 374.64 g of 3 % (w/w) pulp and 749.28 g of demineralized water was mixed in order to obtain 1123.92 g of 1 % (w/w) pulp. Afterwards the pulp was poured into the filtration form for bones and the filtration was started. The filtrations where conducted on A1 and B1. The area of the filtration form for bones were approximately  $280 \text{ cm}^2$ .

## 4.4 Characterization of filtrate

### 4.4.1 Drymattercontent and ashcontent

The filtrate was poured into a preweighed foil form, weighed and placed in an oven at 105 °C for at least 24 hours. After this it was weighed again and placed at 560 °C for at least 12 hours. After this, the form was weighed again to obtain the ash content.

### 4.4.2 Ca<sup>++</sup> content of pulp and filtrate

The Ca<sup>++</sup>-concentration were measured with Atomic Absorption Spectroscopy (Perkin Elmer AAnalyst 100, with Ca Intensitron Lamp and autosampler Perkin Elmer AS-90 plus).

Sample preparation: 2 mL of 3 % (w/w) pulp was mixed with 8 mL of 0.5 M HCl in a 10 mL centrifuge tube for 1 hour before centrifuged at 3500 RPM for 5 minutes.

10 mL of each filtrate is mixed with 400  $\mu$ L 2M HNO<sub>3</sub> for 1 hour in a 10 mL centrifuge tube. Then it was centrifuged at 3500 RPM for 5 minutes.

The samples from both pulp and filtrate was filtrated with 0.45  $\mu$ m syringe filter. The samples were then diluted 1:20.

Standards ranging 0, 2, 4, 6, 8 and 10 mg/L are mixed from a 100 mg/L CA standard for AAS (Fluka) and a 0.1 mL 0.1 M HNO<sub>3</sub>.

## 4.5 Strength analysis of filter cakes

### 4.5.1 Extension

The tensile test machine (Instron Int. Ltd. 5500R) and the software (Merlin) was used for measuring the extension on large filtercakes from two sources, A1 and B1. The flat filtercakes was cut into pieces of 2 cm width. The ends were reinforced with pieces of tape.

The samples were fastened with clamps to the weighing cell (Instron 1 kN pressure/pull) and holder. The set up is illustrated in figure 4.2. The velocity on the analysis was caaried out with an extension of 2 mm/min. During the measurement the force to pull the sample the given length pr. minute was logged.

### 4.5.2 Deformation

With a different set-up on the tensile test machine, the deformation was measured on filter cakes from all five sources.

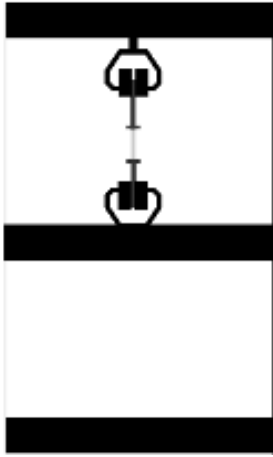


Figure 4.2: Set up for tensile-stress

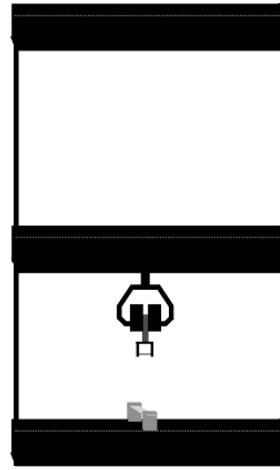


Figure 4.3: Set up for deformation

Set up of the experiment is illustrated in figure 4.3. 6 normal filter cakes of each source were sliced out and the ends were tape reinforced. The sample was fastened in both ends and placed below the pressure cell (Instron) so the pressure would be applied across the sample. The velocity was 10 mm/min. The data being logged was the force to push the sample a given length pr. minute.

# 5. Results

The five paper resources can be divided into two series the A-series and the B-series, which is newsprint and printing paper, respectively. With several filtrations on the same pulp, the first is called take 1, while the second is called take 2. When these filtrations are repeated on other pulps of the same kind in order to validate tendencies and results, they are called 1st repetition and 2nd repetition.

## 5.1 Fibre resources

In order to be able to compare the results from the analysis on the various paper sources it is important to characterize the sources.

### 5.1.1 Drymattercontent and ashcontent

The drymatter content and ash content for the paper sources is shown in table 5.1.

Table 5.1: Drymatter content and ash content for paper resources

Type of paper	Drymatter content [%]	ash content [%]
A1	$91.57 \pm 0.39$	$9.32 \pm 0.32$
A2	$90.60 \pm 0.06$	$8.49 \pm 0.40$
B1	$94.49 \pm 0.18$	$26.63 \pm 0.51$
B2	$95.40 \pm 0.25$	$22.86 \pm 0.99$
B3	$92.97 \pm 0.97$	$17.31 \pm 4.05$

The A-series has a drymatter content of approximately 91 % with less than 10 % ash, while the B-series has a higher drymatter content with an ash content almost twice as high as the A-series.

The drymatter content consist of both an organic part and an inorganic part. This is illustrated in figure 5.1 on the facing page.

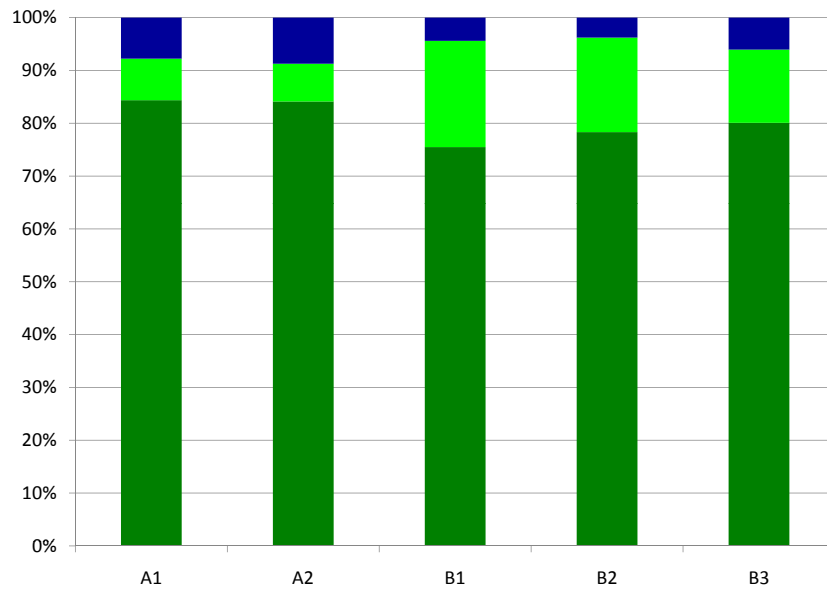


Figure 5.1: ■ is the moisture content, while the drymatter content consists of both ■ and ■, where the light green is the ash content.

Since the ash content is the inorganic part of the drymatter, the part is larger in newspapers. The moisture content can change, since it is dependent on the humidity of the room.

### 5.1.2 Zeta potential

The zeta potential of diluted samples of pulp from each paper resource is measured in order to examine if the fibres have different charge. Also, it is an important criterion to reproduce the experiments.

Table 5.2: Zeta potential in the pulps

Type	Zeta potential [mV]
A1	$-2.8 \pm 0.1$
A2	$-2.6 \pm 0.2$
B1	$-1.8 \pm 0.1$
B2	$-2.5 \pm 0.2$
B3	$-2.5 \pm 0.2$

The zeta potential shows that in neutral tapwater all the fibres are negatively charged, as the potentials are similar except for B1, which is 0.4 mV from the others. The conductivity during measurements of all samples were  $0.534 \pm 0.024 \mu\text{S}$

### 5.1.3 Distribution of Fibre Size

The distribution of the fibres lengths and widths measured on at least 20.000 fibres of each pulp, are shown in the figures 5.2 to 5.11.

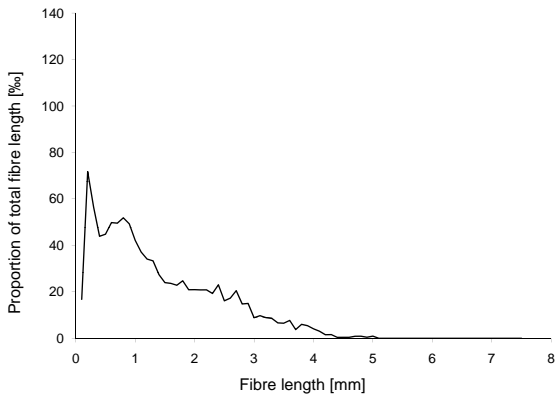


Figure 5.2: Length distribution of A1

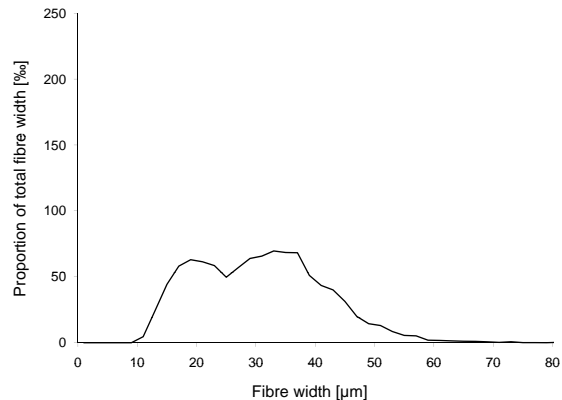


Figure 5.3: Width distribution of A1

For A1, both the length and width distribution shows large spreading. The mean length and width is  $1.39 \pm 1.01$  mm and  $30.71 \pm 10.82$   $\mu\text{m}$ , respectively.

Data for A1 showed that 20 % of fibres in the length distribution are in the range of 0.08 mm to 0.5 mm, while 40 % is between 0.5 and 1.5 mm. 30 % is between 1.5 and 3 mm and the rest is the tail between 3 and 7.5.

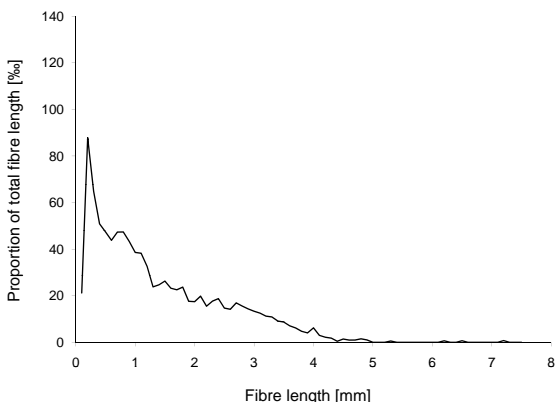


Figure 5.4: Length distribution of A2

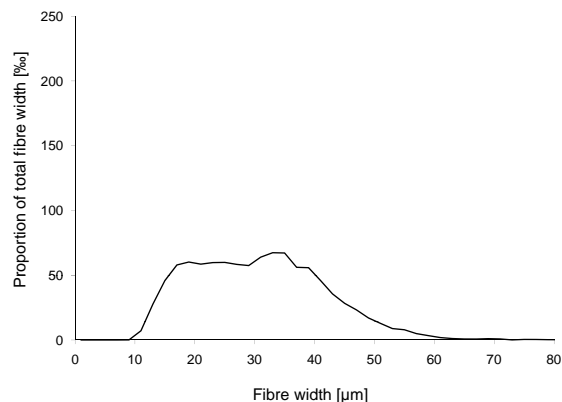


Figure 5.5: Width distribution of A2

The diagrams for length and width of A2 show the same tendency as A1. This is, wide distribution of both length and width. The mean length is determined to be  $1.39 \pm 1.09$  mm, while the mean width is  $30.67 \pm 11.13$   $\mu\text{m}$ . 23 % of the fibres are between 0.08 to 0.5 mm, while approximately 40 % are between 0.5 and 1.5 mm. Between 1.5 and 3 mm 30% of the fibers are present. The tail consists of the the rest between 3 and 7.5 mm.

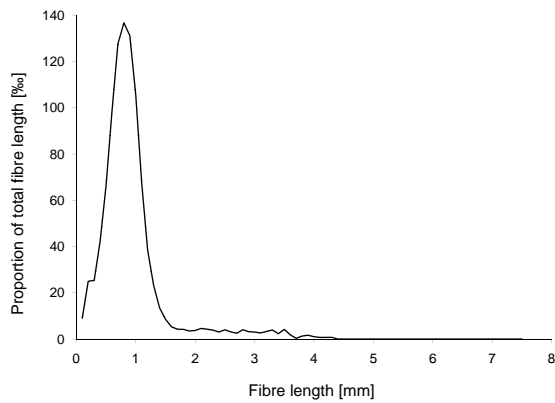


Figure 5.6: Length distribution of B1

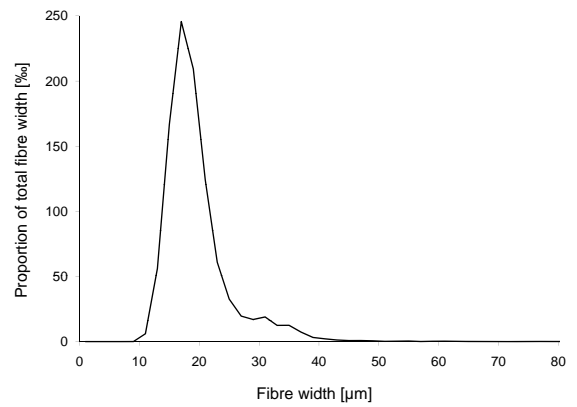


Figure 5.7: Width distribution of B1

The figures for length and width distribution of fibres in B1 show a smaller distribution, than the A-series, but still with a tail to the right. The mean length and width are  $0.94 \pm 0.60$  mm and  $19.5 \pm 5.57$   $\mu\text{m}$ , respectively. The small standard deviations show a narrow distribution of data between the mean values. 24 % are between 0.08 and 0.5 mm, while almost 70 % are in the range 0.5 - 1.5 mm. The last 8 % are the tail running between 1.5 and 7.5 mm.

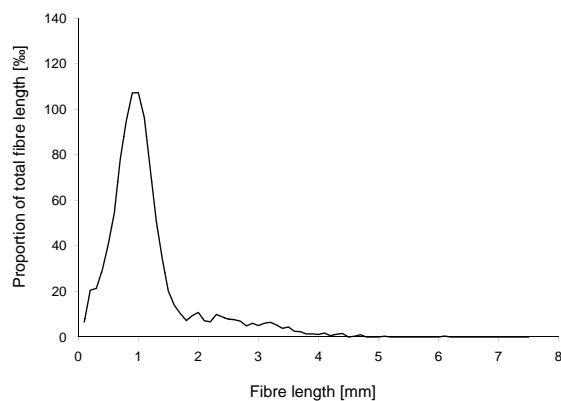


Figure 5.8: Length distribution of B2

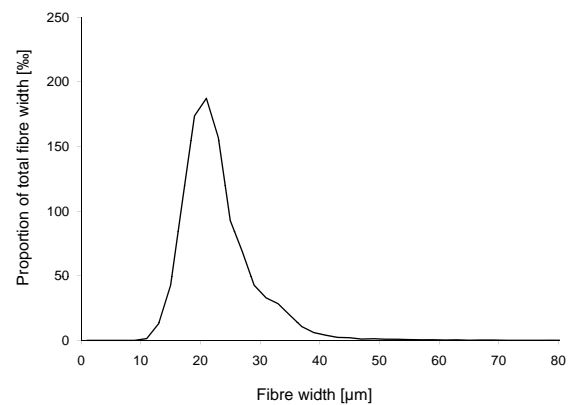


Figure 5.9: Width distribution of B2

The length and width distribution of fibres from B2 show the same tendency as with B1 i.e. narrow distribution of data. Mean length and width are  $1.17 \pm 0.74$  mm and  $22.93 \pm 6.11$   $\mu\text{m}$  respectively. Only 15 % of fibres are between 0.08 and 0.5 mm, while 70 % are between 0.5 and 1.5 mm. In the range of 1.5 to 3.0 mm there are 12 %. The rest is the tail between 3.0 and 7.7 mm.

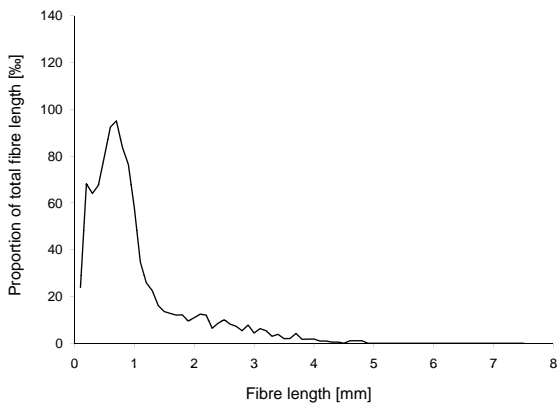


Figure 5.10: Length distribution of B3

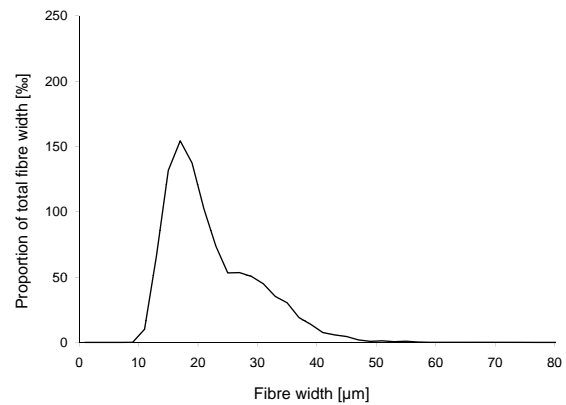


Figure 5.11: Width distribution of B3

The length distribution of B3 is more similar to the A-series, since there is an extra top between 0.08 and 0.5 mm. The width distribution is on the other hand more similar to the others in the B-series. Mean length and width are  $1.00 \pm 0.82$  mm and  $22.20 \pm 7.59$   $\mu\text{m}$ , respectively. 33 % of fibers are in the range between 0.08 and 0.5 mm. 50 % are between 0.5 and 1.5, while 15 % are between 1.5 and 3.0 mm, the rest is the tail between 3 and 7.5 mm.

The fraction of fines in all samples are also found, as shown in table 5.3.

Table 5.3: Percentage of fines in the various pulps.

Type	Fraction of fines [%]
A1	13.2
A2	15.5
B1	6.5
B2	7.5
B3	15.8

A fine is determined if the ratio between length and width is lower than 4. Both A-series and B3 have more than 10 % of fines, while B1 and B2 only have half the amount of that.

### 5.1.4 Calculation of specific surface of mean fibres

Based on the mean length and width of the fibres, the specific surface,  $S_o$ , are estimated from equation 2.21 on page 12.  $S_o$  are lowest for the A1 and A2 with  $131.71 \pm 61.79$  and  $131.87 \pm 64.00$   $\text{mm}^{-1}$ . The B-series have higher  $S_o$ -values at  $207.31 \pm 49.79$   $\text{mm}^{-1}$ ,  $176.15 \pm 44.08$   $\text{mm}^{-1}$  and  $182.14 \pm 63.25$  for B1, B2 and B3, respectively.

## 5.2 Filtrations on the paper ressources

The pressure curves shown is the mean pressure. The pressure curve is meaned over 10 data points. A1 filtrated 4 times is shown in figure 5.12.

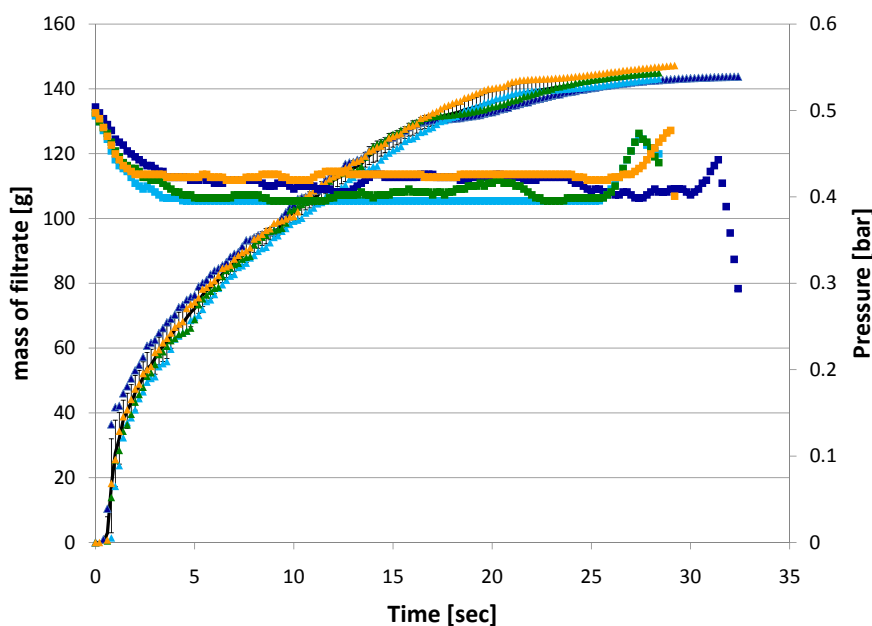


Figure 5.12: Filtration and pressure curve of A1. ■ is the pressure curve from take 1 and ▲ is the matching filtrate curve. — is the mean filtration curve. Take 2 is illustrated in ■, take 3 is ■ and take 4 is ■.

The curves of the various takes are similar. At the end of the filtration, the mass is still increasing. The mass-curve increases slowly and steadily. The pressure curve decreases fastly and levels out, the level line is not linear. This is because the pressure transducer measures in intervals. When the pressure starts to increase again, the vent is shot and vacuum is rebuild. The estimated filtration time is 28 seconds. The error lines from the mean filtration curve is hidden below the filtration curves from the different takes.

B1 filtrated 4 times shown in figure 5.13 on the following page

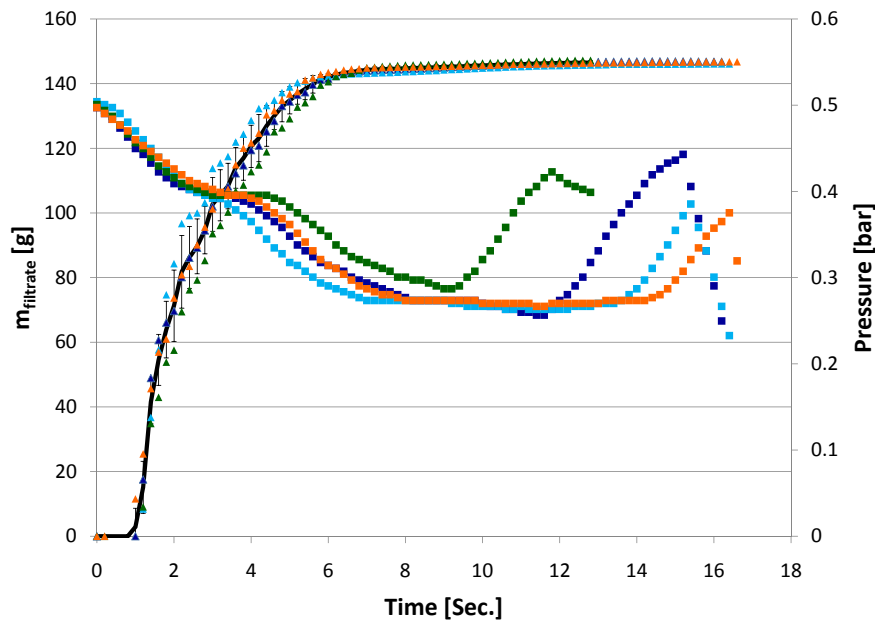


Figure 5.13: Filtration and pressure curve of B1.  $\blacksquare$  is the pressure curve from take 1 and  $\blacktriangle$  is the matching filtrate curve.  $\text{—}$  is the mean filtration curve. Take 2 is illustrated in  $\blacksquare$ , take 3 is  $\blacksquare$  and take 4 is  $\blacksquare$ .

The pressure curve for B1 is different from the pressure curve for A1. First it has a fast decrease as A1, but instead of leveling out, there is a bump, after which it decreases again before leveling out. Since the filtration is faster, the pressure curve is not all levelled out. Estimated time of filtration is 5 seconds.

Each five selected cellulosic resources was filtrated 4-6 times and the following correlation, shown in figure 5.14 on the next page, appeared. The curves are means of the 4-6 filtrations of each pulp.

The B-series show similar tendencies, while the dewatering of A-series takes longer time. The A-series are similar to figure 5.12 on the preceding page, while the B-series are similar to the figure 5.13.

In order to validate the data and determine if they are reproducible, the filtrations were repeated twice, as shown in figure 5.15 on the facing page and 5.16 on the next page.

For the 1<sup>st</sup> repetition, the same tendency of filtration is shown, but only faster than in 5.14 on the facing page. The filtrations in 2<sup>nd</sup> repetition, figure 5.16 on the next page, show the same tendency as the 1<sup>st</sup> repetition was made. A-series are slower to dewater than the B-series.

Table 5.4 shows the data from the various filtrations. Mass of pulp:  $m_{pulp}$  is the amount of pulp weighed to the specific take. Mass of filtrate:  $m_{filtrate}$  is the highest value of the data logged. Mass of wet filtercake from the specific take:  $m_{cake,w}$ . The drymatter content of the filtercakes: DM Cake. The difference is the difference between:  $m_{pulp} - (m_{filtrate} + m_{cake,w})$

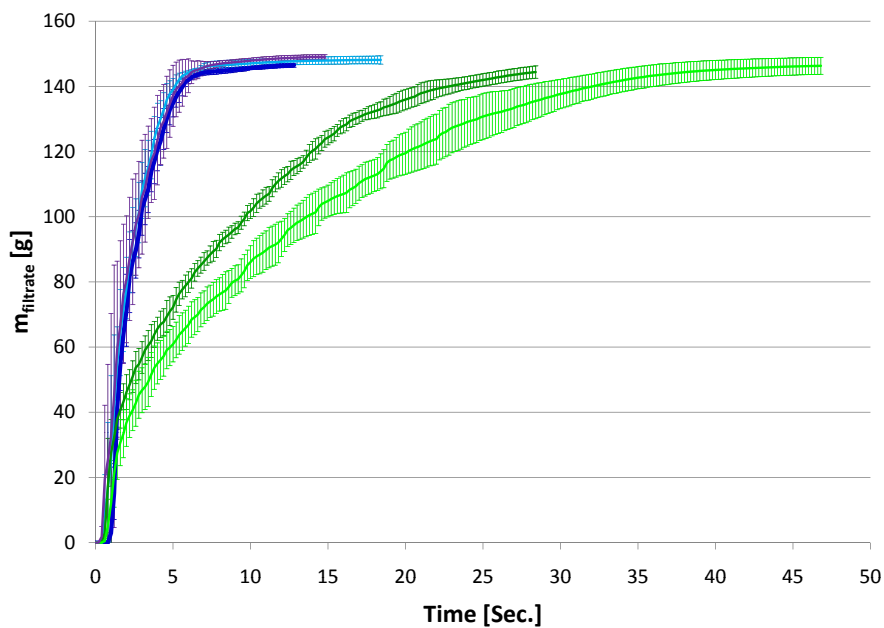


Figure 5.14: Filtration curve of cellulosic ressources. — is A1, — A2, — B1, — B2, and — B3

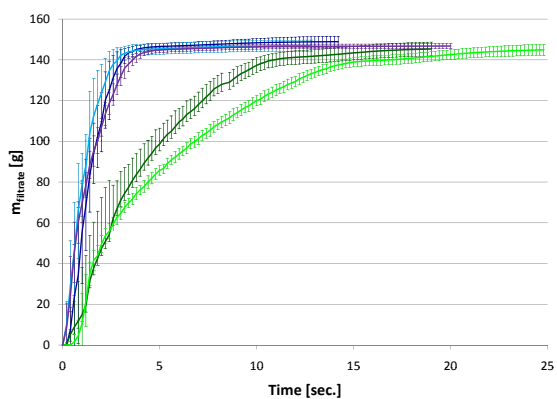


Figure 5.15: Filtration curve of cellulosic ressources. 1<sup>st</sup> repetition. — is A1, — A2, — B1, — B2, and — B3.

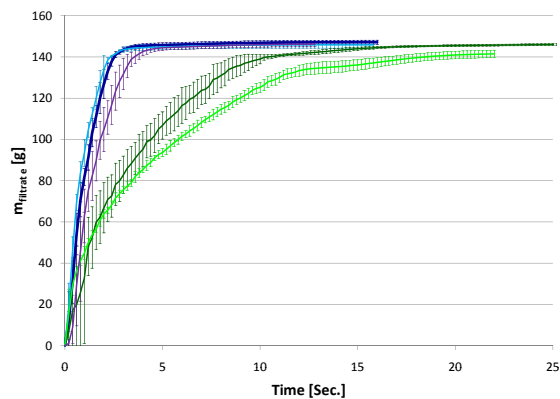


Figure 5.16: Filtration curve of cellulosic ressources. 2<sup>nd</sup> repetition. — is A1, — A2, — B1, — B2, and — B3.

Table 5.4: Mass of filtrate and wet cake compared to Drymatter content and mass of pulp.

Type	$m_{pulp}$ [g]	$m_{filtrate}$ [g]	$m_{cake,w}$ [g]	DM cake [%]	difference [g]
A1 1	154.32	143.75	7.27	20.91	3.3
A1 4	157.32	147.13	7.86	19.85	2.33
A1 1	154.23	145.8	6.83	21.67	1.6
A1 3	154.8	138.7	6.86	22.16	9.24
A1 5	154.41	146.77	6.51	23.81	1.13
A2 1	154.7	142.95	6.93	22.94	4.82
A2 5	156.65	148.11	7.4	21.49	1.14
A2 1	154.35	143.78	6.85	22.77	3.72
A2 3	154.42	142.4	7.04	21.73	4.98
A2 5	154.58	146.38	6.99	21.89	1.21
B1 2	154.12	147.71	4.78	25.73	1.63
B1 3	154.51	145.69	5.32	25.56	3.5
B1 5	154.17	149.16	5.28	25.38	-0.27
B1 2	154.28	148.27	5.14	25.10	0.87
B1 3	154.34	148.14	5.14	25.10	1.06
B1 5	154.41	145.94	5.26	25.86	3.21
B2 1	154.79	148.08	5.72	22.35	0.99
B2 4	154.4	145.92	5.51	23.73	2.97
B2 1	154.04	144.81	5.95	23.85	3.28
B2 4	154.29	147.86	5.9	27.10	0.53
B2 6	154.1	147.65	6.08	25.77	0.37
B3 1	154.06	144.67	5.43	26.52	3.96
B3 3	154.53	147.63	5.53	26.40	1.37
B3 5	154.14	147.2	5.7	26.32	1.24
B3 1	154.2	146.22	5.34	26.03	2.64
B3 3	154.07	147.11	5.25	25.33	1.71
B3 5	154.41	144.67	5.63	25.75	4.11

For the A-series the drymatter content of the filter cake is  $21.68 \pm 1.48$  g, while the mean  $m_{filtrate}$  is  $144.43 \pm 3.46$  g for A1, while the mean drymatter content and mean  $m_{filtrate}$  for A2 is  $22.17 \pm 6.65$  and  $144.72 \pm 2.43$  g, respectively. The mean drymatter content on filtercakes and mean  $m_{filtrate}$  from B1 is  $25.45 \pm 0.32$  g and  $147.49 \pm 1.38$  g. For B2 the mean drymatter content and mean  $m_{filtrate}$  is  $24.56 \pm 0.32$  g and  $146.86 \pm 1.43$  g. The

mean drymatter content in filtercakes from B3 is  $26.06 \pm 0.45$  while the mean  $m_{filtrate}$  is  $146.25 \pm 1.31$  g. Less  $m_{filtrate}$ , less drymatter content in the filtercakes. The standard deviations are larger for the A-series than the B-series.

Figure 5.17 shows the filtration time estimated from figures 5.14-5.16.

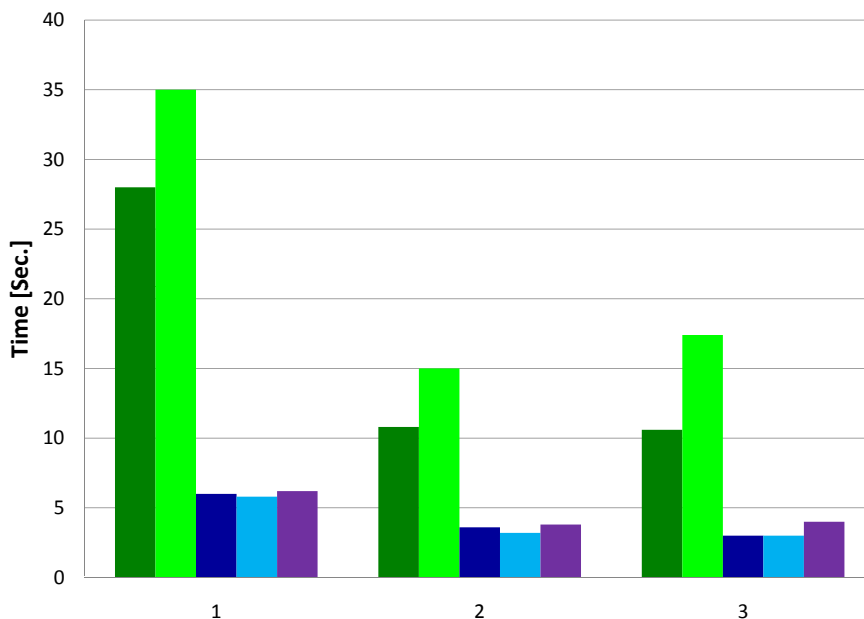


Figure 5.17: Filtration time of the various experiments. 1 is the first filtration series, while 2 and 3 are the 1<sup>st</sup> and 2<sup>nd</sup> repetition, respectively. ■ A1, ■ A2, ■ B1, ■ B2, ■ B3.

The filtration of the various pulps is completed in the same order. There is no relationship between the filtration time from the various filtration besides that they are completed in the same order.

The data logged in the filtrations can, by using equation 2.7 on page 10, create a Ruth Plot, plotting  $\frac{dt}{dV}$  versus  $\frac{V}{P}$ . An example is shown in figure 5.18, the rest is in Appendix Ruth plot on the enclosed CD-rom .

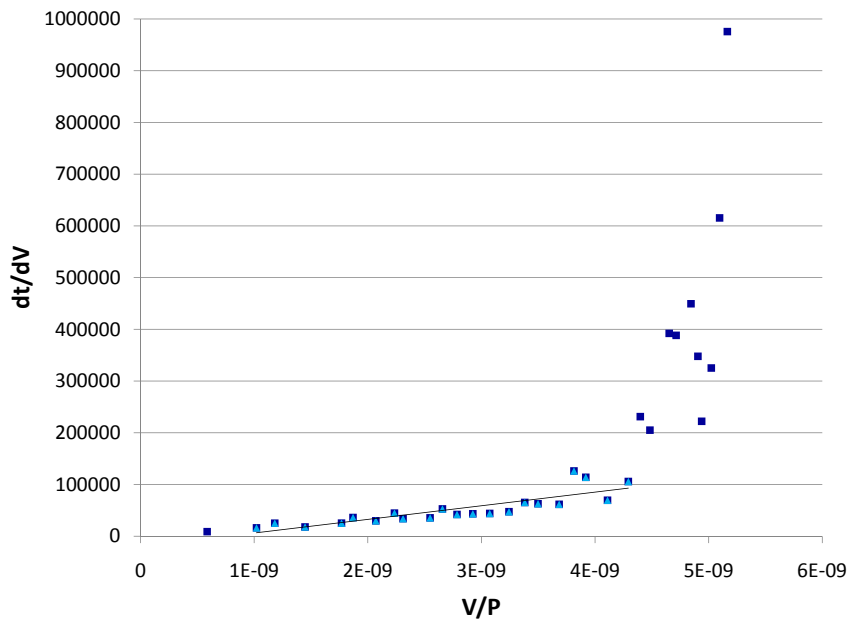


Figure 5.18: Ruth plot of B3, ■ filtration ▲ part which has the following linearity  $\frac{dt}{dV} = 2.64x10^{13} - 2.01\frac{V}{P}$   $R^2=0.71$

The slope is used to calculate  $\alpha$  for each filtercake. The mean  $\alpha$  is shown in figure 5.19.

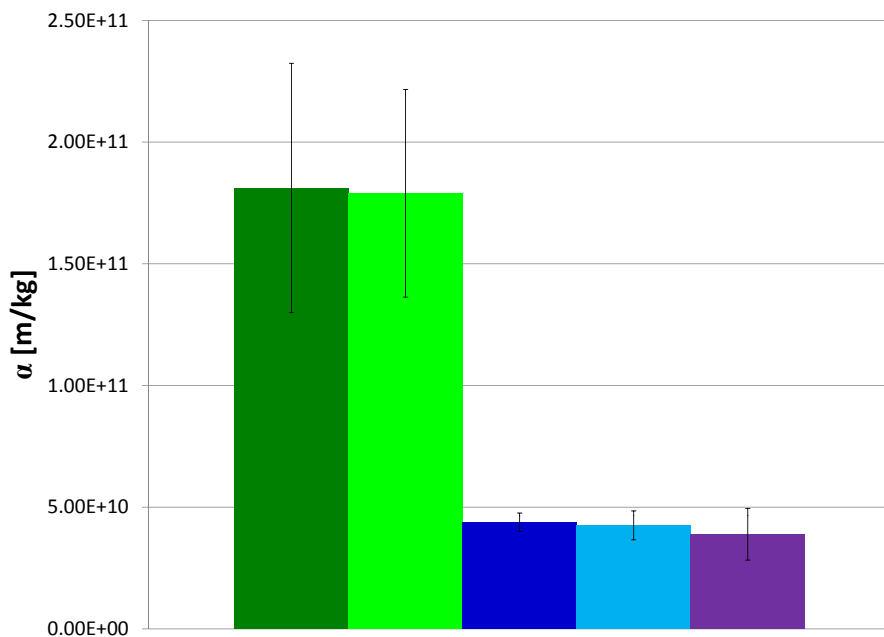


Figure 5.19:  $\alpha$ -values for the first filtrations. ■ A1, ■ A2, ■ B1, ■ B2, ■ B3.

As showed in figure 5.19 there is an obviously difference between A-series and B-series. The A-series has higher  $\alpha$ -values with larger standard deviations, than the B-series. In order to examine if the results are reproducible the following results are shown:

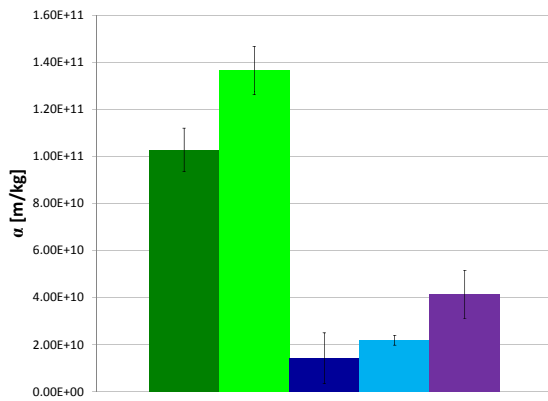


Figure 5.20:  $\alpha$ -values for 1<sup>st</sup> repetition. ■ A1, ■ A2, ■ B1, ■ B2, ■ B3.

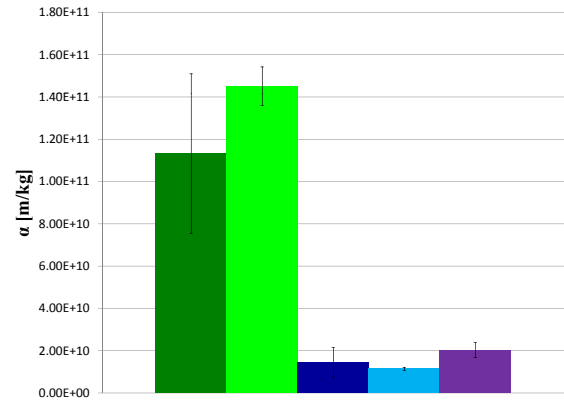


Figure 5.21:  $\alpha$ -values for 2<sup>nd</sup> repetition. ■ A1, ■ A2, ■ B1, ■ B2, ■ B3.

The data were not reproducible, but the same tendency is present.

### 5.3 Concentration of $\text{Ca}^{++}$ in pulp and filtrate

The concentration of  $\text{Ca}^{++}$  in pulp and filtrate is determined and shown in table 5.5.

Table 5.5:  $\text{Ca}^{++}$ -concentration in pulp and filtrate

Type	Conc. in pulp [mg]	Conc. in filtrate [mg]	$\frac{C_{filtrate}}{C_{pulp}}$ [%]
A1	317	39	12
A2	244	49	20
B1	1034	207	20
B2	981	192	20
B3	892	166	19

When comparing the  $\text{Ca}^{++}$ -concentration in the filtrate with the one in the pulp there is a proportion between them of 20 %, except with A1, which is only 12 %. This indicates that there is a better retention of  $\text{Ca}^{++}$  in the filter cakes from A1. There is more calcium in the B-series than in the A-series, but printing paper is more bright white than newspaper, which can be caused by  $\text{CaCO}_3$ .

### 5.4 Strength analysis

Strength analysis was performed on filter cakes from both A1 and B1. The filter cake were the large filter cakes and they are called bones.

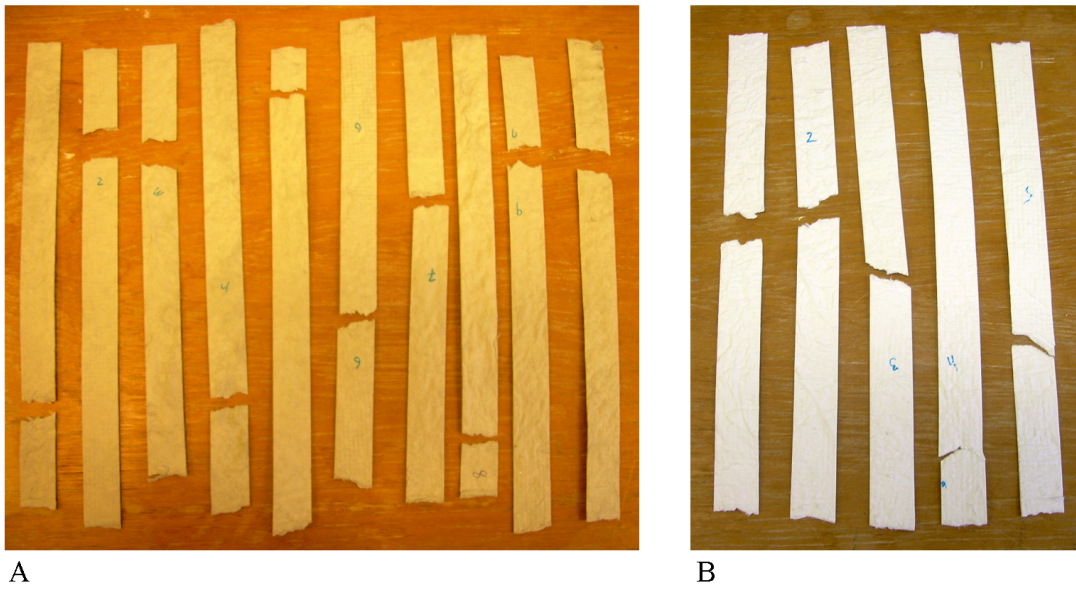


Figure 5.22: A: Illustration of the breaks of bones from A1. B: Illustration of the breaks of bones from B1.

An illustration of the breaks of bones is presented in 5.22 A and B for A1 and B1, respectively. The pieces are put together so they will fit if hold together. The breaking are not linear and the tearing can happen in a wide angle in the depth of the bone.

Table 5.6: Mass and size of the bones.

Type of sample	Mass of sample [g]	Width [cm]	length [cm]	Thickness [mm]	Observation
A1 1	1.94	2.0	25.2	$1.71 \pm 0.15$	
A1 2	1.86	2.0	25.1	$1.67 \pm 0.23$	
A1 3	1.56	2.0	22.5	$1.81 \pm 0.47$	
A1 4	2.09	2.0	26.5	$1.77 \pm 0.24$	
A1 5	1.96	2.0	26.0	$1.50 \pm 0.17$	Break in tape
A1 6	2.26	2.0	25.2	$1.73 \pm 0.21$	Slipped in tape
A1 7	2.07	2.0	25.0	$1.82 \pm 0.12$	
A1 8	2.08	2.0	28.5	$1.89 \pm 0.12$	Break in tape
A1 9	1.71	2.0	25.4	$1.49 \pm 0.21$	
A1 10	1.94	2.0	25.6	$1.47 \pm 0.16$	
B1 1	1.84	2.0	22.5	$1.37 \pm 0.29$	
B1 2	1.69	2.0	22.1	$1.54 \pm 0.21$	
B1 3	1.94	2.0	24.2	$1.21 \pm 0.18$	
B1 4	2.36	2.0	25.5	$1.26 \pm 0.22$	Break in tape
B1 5	1.86	2.0	23.4	$1.00 \pm 0.23$	

As shown in table 5.6 on the facing page the samples measured were not similar in size. These length and width measurements were performed with vernier caliper. For A1, the mean length and mean mass is  $25.5 \pm 1.49$  cm and  $1.95 \pm 0.20$  g, respectively. For B1 the mean length and mean mass is  $23.54 \pm 1.36$  cm and  $1.94 \pm 0.25$  g.

The four samples which did break in the tape or slipped in the tape are not being taking into consideration in the further calculations. They are shown in red in figures 5.23 and 5.24.

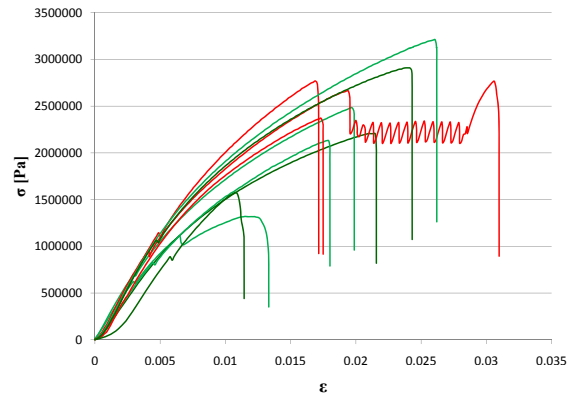


Figure 5.23: Stress-strain curve for A1. The red ones are A1 5, A1 6 and A1 8.

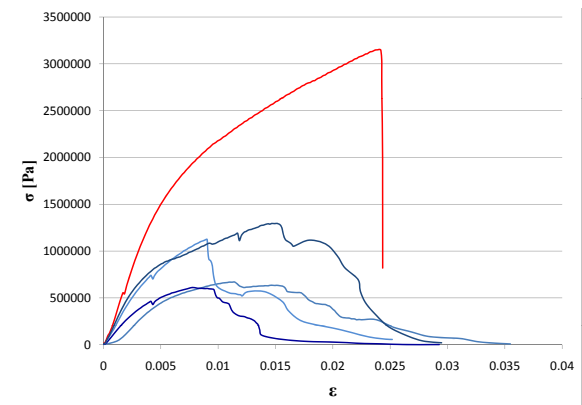


Figure 5.24: Stress-strain curve for B1. The red one are B1 4.

Here the stress strain curves from the tensile stress test are shown for A1 and B1. Even though, there is no clear correlation between the various takes of A1, the shape of the curves are similar, even though the max load is not the same. They all have a sharp break, whereafter a sharp decrease in  $\sigma$  occurs. This could imply the material is brittle. The B-series, on the other hand, does not have the same sharp decrease. This could imply that the printing paper is not as brittle as the newspaper.

All curves starts the same way in the two figures. Young's modulus is calculated for them all in this linear range and shown in table 5.7.

Table 5.7: Young's modulus on the bones.

<b>Type of sample</b>	A1 1	A1 2	A1 3	A1 4	A1 5
<b>E [Pa]</b>	$2.12 \cdot 10^8$	$1.79 \cdot 10^8$	$1.97 \cdot 10^8$	$2.40 \cdot 10^8$	-
<b>Type of sample</b>	A1 6	A1 7	A1 8	A1 9	A1 10
<b>E [Pa]</b>	-	$2.19 \cdot 10^8$	-	$2.51 \cdot 10^8$	$2.05 \cdot 10^8$
<b>Type of sample</b>	B1 1	B1 2	B1 3	B1 4	B1 5
<b>E [Pa]</b>	$1.02 \cdot 10^8$	$1.16 \cdot 10^8$	$1.86 \cdot 10^8$	-	$1.94 \cdot 10^8$

The smallest E-values from A1 are similar to the large E-values from B1. The Young's modulus is illustrated for both A1 and B1, in figure 5.25 on the following page.

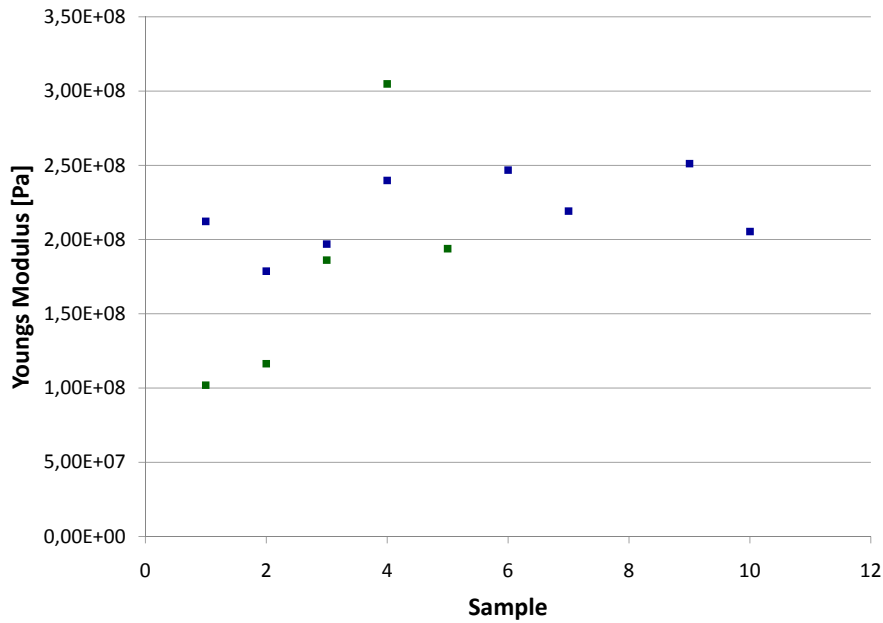


Figure 5.25: Young's modulus from the strength analysis of the bones from ■ A1 and ■ B1.

As shown, the uncertainties are too large to give a final answer, since the data for A1 is overlapped by the results from B1 but the tendency is that there is more strength in the cuts from A1 than in the cuts from B1.

Instead, the max load is found for both A1 and B1. This is shown in table 5.8.

Table 5.8: Max load of the bones from A1 and B1.

Type of sample	Max load [Pa]
A11	$1.32 \times 10^6$
A12	$2.21 \times 10^6$
A13	$2.13 \times 10^6$
A14	$2.48 \times 10^6$
A15	-
A16	-
A17	$3.21 \times 10^6$
A18	-
A19	$2.91 \times 10^6$
A110	$1.58 \times 10^6$
B11	$6.70 \times 10^5$
B12	$6.10 \times 10^5$
B13	$1.12 \times 10^6$
B14	-
B15	$1.30 \times 10^6$

The maximum load the samples could handle was read from the figures 5.23 and 5.24 on page 35, and the difference was that the newsprint could resist a higher pull before it broke. The max load for A1 is  $2.26 \times 10^6 \pm 6.76 \times 10^5$  Pa, while max load for B1 is  $9.25 \times 10^5 \pm 3.37 \times 10^5$  Pa.

### 5.4.1 Deformation

The deformation experiment gave the following observations:

Table 5.9: Overview of the bending results on the filter-cakes.

Type	Observation
A1 2	Bend and broke
A1 4	Bend and broke another place
A1 6	Bend
A1 1	Bend
A1 2	Bend
A1 3	Bend
A2 2	Bend and broke in two
A2 4	Bend and broke another place in tape
A2 6	Bend and broke in two
A2 1	Bend and broke
A2 2	Bend and broke in two
A2 3	Bend
B1 1	Bend
B1 2	Bend
B1 6	Bend and broke another place
B1 2	Bend and broke in two
B1 4	Bend and broke another place in tape
B1 6	Bend and broke another place in tape
B2 1	Bend
B2 2	Bend
B2 6	Bend and broke another place
B2 2	Bend
B2 3	Bend and broke where tighten
B2 4	Bend
B3 1	Bend and broke another place
Continued on next page	

**Table 5.9 – continued from previous page**

Type	Observation
B3 4	Bend and broke
B3 6	Bend and broke another place in tape
B3 2	Bend
B3 4	Bend and broke
B3 6	Bend and broke another place

Few samples broke in the tape, so the stresses from these can be false. Therefore, they are not included in the following treatment of data. Several samples only bent instead of breaking, while other did both either in the same place or different places.

The following figure is an illustration of the stress-strain curve for the bending experiments with A1 and B1.

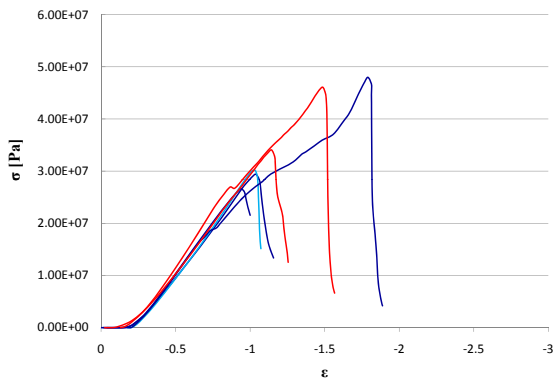


Figure 5.26: Stress-strain correlation of A1 bending tests.

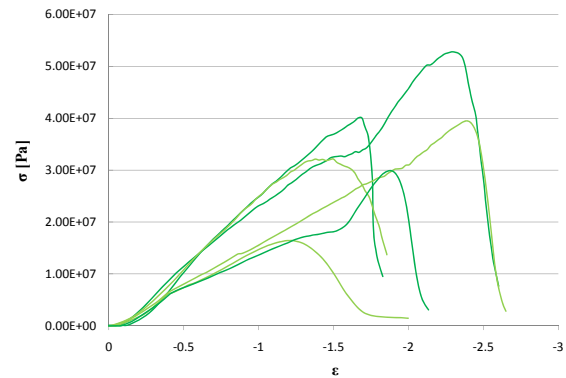


Figure 5.27: Stress-strain correlation of B1 bending tests.

The curves show an increase in stress, as the strain increases. At a certain strain, the stress starts to fall rapidly, indicating bending or breaking of the cakes. There is no significant difference in maximum strain between the paper sources. The figures though, show that the strain, where the bending occurs, is higher for the A-series than the B-series.

The E-values for the deformation test is shown in figure 5.28 on the facing page.

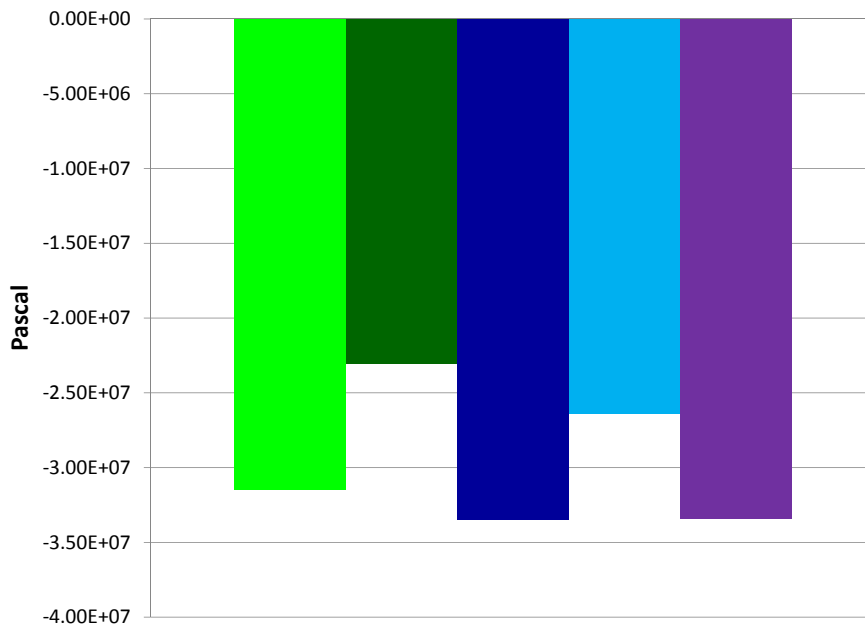


Figure 5.28: ■ is the mean E-value for B1, ■ B2, ■ B3, and ■ is the E-value for A1, while ■ is for A2.

Figure 5.28 shows that there is no significant difference in the E-values between the paper sources. This means, that there is a difference in the forces affecting the pulling resistance and the pushing resistance.

## 5.5 Variation experiment

During the experiment of mixing the two selected pulps together in order to examine if there were a better mixture, the results are as illustrated in figure 5.29.

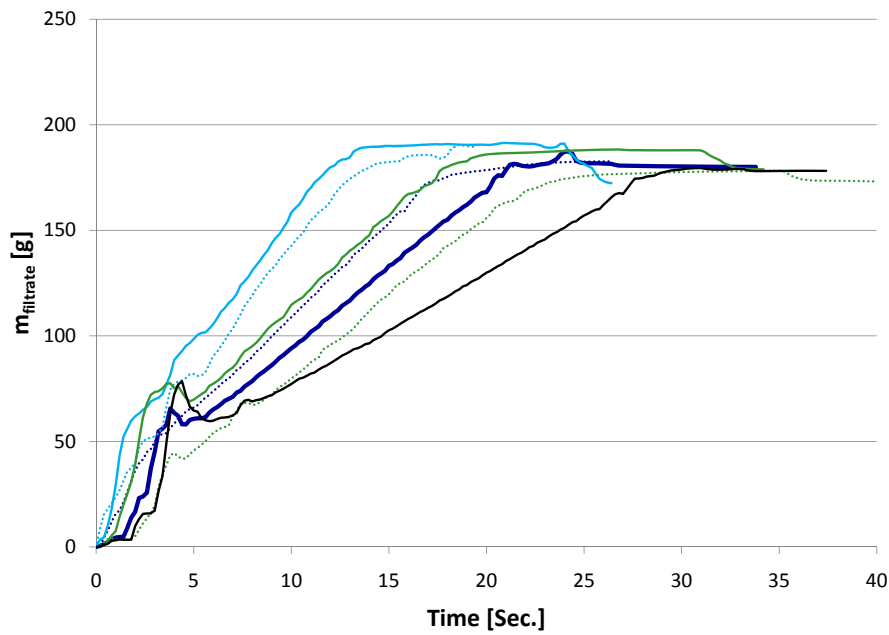


Figure 5.29: Mean filtration curves for mixing experiments. — for 0:100, ..... for 10:90, — for 30:70, ..... for 50:50, — for 70:30, ..... for 90:10, — for 100:0

The different curves in figure 5.29 all show a bumpy start, followed by a steadier filtration, this is caused by the alternative set-up. The steeper the line, the faster the filtration. The correlation between A1-content and filtration time is shown in figure 5.30.

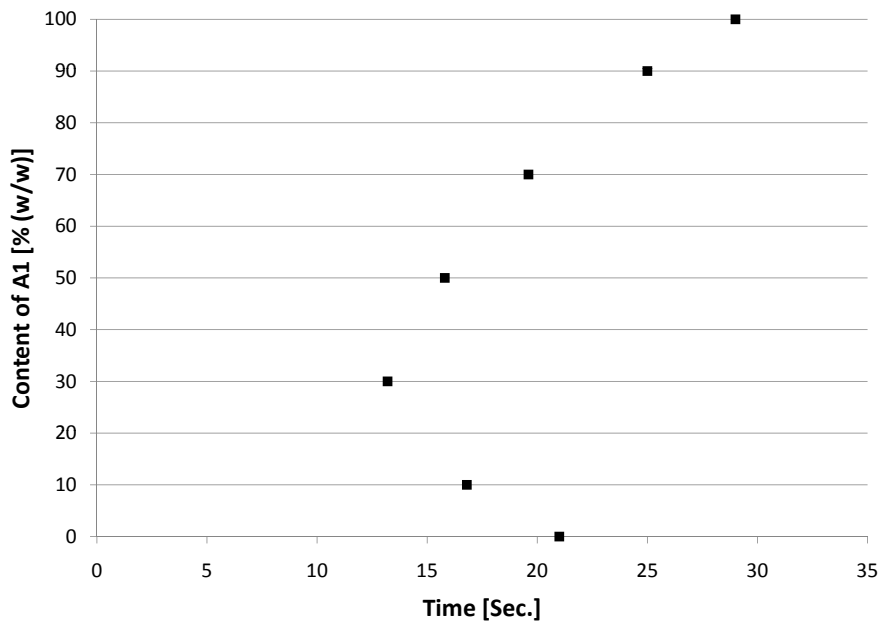


Figure 5.30: Dewatering time vs. mixing grade

The results from figure 5.30 show that the dewatering is not linear when compared to the content of A1. The fastest filtration is the one with 30:70.

In table 5.10 the mass of pulp:  $m_{pulp}$  is the amount of pulp weighed to the specific take. Mass of filtrate:  $m_{filtrate}$  is the mass of filtrate weighed. Mass of wet filtercake from the specific take:  $m_{cake,w}$ . The drymatter content of the filtercakes: DM Cake. The difference is the difference between:  $m_{pulp} - (m_{filtrate} + m_{cake,w})$ .

Table 5.10: Mass of filtrate and wet cake compared to Drymatter content and mass of pulp.

Type	$m_{pulp}$ [g]	$m_{filtrate}$ [g]	$m_{cake,w}$ [g]	DM cake [%]	difference [g]
0:100 1	154.55	145.69	5.82	23.71	3.04
0:100 2	154.00	146.92	5.88	21.43	1.20
10:90 1	154.46	145.06	6.08	24.84	3.32
10:90 2	154.79	144.70	6.26	23.80	3.83
10:90 3	156.06	146.27	5.82	24.05	3.97
30:70 1	156.82	144.80	6.42	24.61	5.60
30:70 2	154.19	144.80	6.18	24.60	3.21
30:70 3	156.46	146.99	6.14	24.43	3.33
50:50 1	154.16	144.58	6.49	23.88	3.09
50:50 2	154.00	143.73	6.59	23.52	3.68
50:50 3	154.81	146.75	6.45	23.72	1.61
70:30 1	154.77	143.69	6.88	22.24	4.02
70:30 2	155.13	144.79	6.71	22.65	3.63
70:30 3	156.37	146.20	6.94	21.33	3.23
90:10 1	154.24	144.46	7.73	20.96	2.05
90:10 2	154.45	143.78	7.47	21.69	3.20
90:10 3	154.16	144.10	7.53	21.38	2.53
100:0 1	155.53	144.99	8.04	19.03	2.50
100:0 2	155.85	146.31	7.87	21.22	1.67

The difference in conservation of mass is acceptable in all situations. The large indifference with 30:70 is caused by the filtrate from take 1 and 2 was mixed up and therefore the results is meaned and by that skewed.

With the mix of 0:100 mean  $m_{filtrate}$  is  $146.31 \pm 0.87$  and the meaned drymatter content of cake is  $22.57 \pm 1.61$ . While the 10:90 mixture had a mean  $m_{filtrate}$   $145.34 \pm 0.82$  and a meaned DM cake on  $24.23 \pm 0.54$ , the 30:70 mixture had a mean  $m_{filtrate}$   $145.53 \pm 1.26$  and a meaned DM cake on  $24.55 \pm 0.10$ . For the mixture of 50:50 the mean  $m_{filtrate}$  an DM cake is  $145.02 \pm 1.56$  and  $23.71 \pm 0.18$  respectively. The mixture of 70:30 had

a mean  $m_{filtrate}$  on  $144.89 \pm 1.26$  and DM cake on  $22.07 \pm 0.68$ . The mix consisting of 90:10 had a meaned  $m_{filtrate}$  on  $144.11 \pm 0.34$  and a DM cake on  $21.34 \pm 0.37$ . Finally the mixture of 100:0 had the mean  $m_{filtrate}$  an DM cake is  $145.65 \pm 0.93$  and  $20.12 \pm 1.55$  respectively.

Between the meaned  $m_{filtrate}$  and meaned DM cake the connection is clear, the higher the  $m_{filtrate}$  the higher the DM cake.

Estimated guess on fiber lenght distribution is illustrated in figure 5.31. The estimation is based on the length of fibres in figures 5.2 and 5.6.

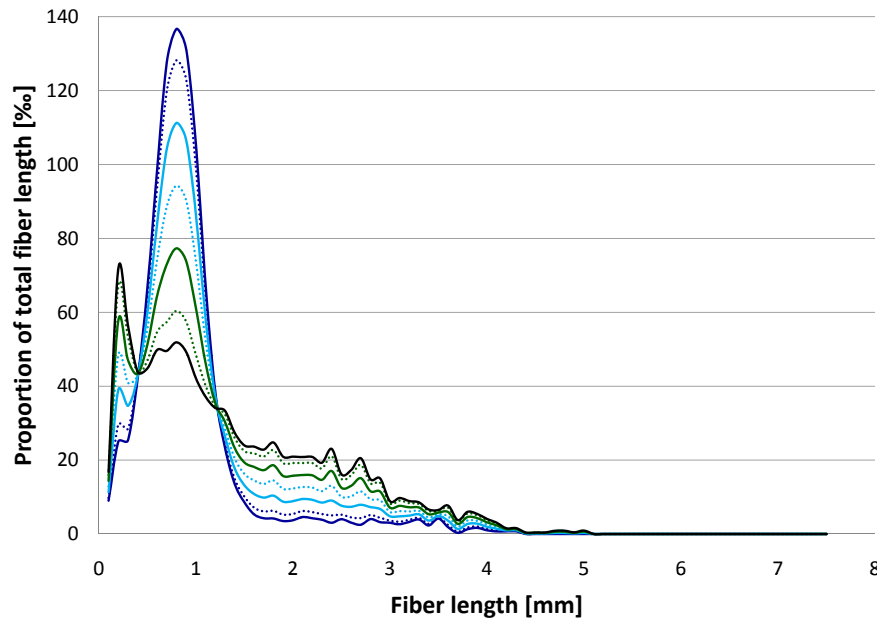


Figure 5.31: Estimate of the fiber length distribution of the various mixtures of pulp. — for 0:100, ..... for 10:90, — for 30:70, ..... for 50:50, — for 70:30, ..... for 90:10, — for 100:0

The faster the dewatering the larger the gaps or the larger the fibers, the slower the dewatering the smaller the gaps and fibers. The fastest dewatering is not the one with the smallest distribution of fibers. The mean length for the various mixtures is as follows: The mean length of the various mixtures were  $0.99 \pm 0.67$  mm,  $1.08 \pm 0.78$  mm,  $1.17 \pm 0.86$  mm,  $1.26 \pm 0.93$  mm and  $1.35 \pm 0.99$  mm for 10:90, 30:70, 50:50, 70:30 and 90:10, respectively.

## 6. Discussion

In order to compare the data from the various filtrations, the mass of pulp weighed has to be similar. The mean  $m_{pulp}$  of all filtrations is  $154.56 \pm 0.90$  g. This means, there is a derivation in percent on 0.6 %. This implies that the difference measured between the pulps has nothing to do with the difference in the sample for the analysis.

**Comparison of characterization of fibres** Since the repulsive forces between the fibres are small (Table 5.2 on page 23), the only effect one might expect is a faster dewatering, since the small repulsion makes it possible for the particles to aggregate. The filtrations are performed in demineralized water, which means, that no ions are present to neutralize the negatively charged fibres. Aggregation can have the effect to create a poorer dewatering, and thereby maintain a higher moisture content in the filter cakes.

The mean lengths of A1 and A2 are  $1.39 \pm 1.01$  mm and  $1.39 \pm 1.09$  mm. The mean lengths of B1, B2 and B3 are  $0.94 \pm 0.60$  mm,  $1.17 \pm 0.74$  mm and  $1.00 \pm 0.82$  mm (Subsection 5.1.3 on page 24). This shows, a larger mean length of the fibres in the A-series. Though, the paper sources with the highest amount of fibres in the lower range of 0.08 - 0.50 mm, are the A-series, while the B-series has the highest amount of fibres in the range of 0.50 - 1.50 mm. This is explained by the higher distribution of fibre lengths of the A-series, compared to the B-series. The same tendencies are observed for the fibre widths. This means, that the A-series have a higher fibre width with a higher distribution, compared to the fibres from the B-series.

In both A1, A2 and B3 there is almost twice as much fines as in B1 and B2 (Table 5.3 on page 26). B1 and B2 is produced by chemical pulping which should have the effect to minimize the content of fines, when compared to mechanical pulping (Subsection 2.1.3 on page 5 and 2.1.3 on page 6). A1 and A2 is produced from mechanical pulping and can furthermore contain recycled fibres (Section 3.1 on page 15). In order to reuse recycled fibres, the fibres are often beaten which increases the amount of fines. The high content of fines in B3 is unexpected, since it in theory should look similar to B1 and B2. One explanation can be the definition of fines, fibres with a length to width ratio smaller than 4. The length distribution of B3 is more similar to the A-series, while the width distribution is similar to the others of the B-series. This could also explain the high content of fines in A-series, as the probability of fines increases if the fibres are shorter.

Since the pulping carried out in these experiments are similar, the difference in fines is

pre-existing. A lower strength of the fibres could have caused them to break easier during the treatments, and therefore give a higher amount of fines.

Since the A-series was mechanically pulped, no effort was made in order to remove either the hemicellulose or the lignin. This could also have an effect on the pulp.

Fibres below the length of 80  $\mu\text{m}$  are not measured.

From the mean lengths and widths of the fibres,  $S_o$  is estimated from equation 2.22 on page 12 to be higher for the B-series than the A-series. This is because, the average fibres are longer and wider in the A-series than in the B-series, giving a lower ratio of area of surface to volume. From equation 2.20 on page 11 it is given, that higher  $S_o$  gives lower flux through the filter cakes.

The B-series has mean  $S_o$ -values at  $207.31 \pm 49.79 \text{ mm}^{-1}$ ,  $176.15 \pm 44.08 \text{ mm}^{-1}$  and  $182.14 \pm 63.25 \text{ mm}^{-1}$  for B1, B2 and B3, respectively. The A-series have lower  $S_o$ -values at  $131.71 \pm 61.79 \text{ mm}^{-1}$  and  $131.87 \pm 64.00 \text{ mm}^{-1}$  for A1 and A2, respectively. According to Kozeny-Carman this should mean, that the A-series is faster to dewater than the B-series. However this is not the case, since the filtration time is higher on the A-series than the B-series. The mean length and width has large standard deviations, especially at the A-series and therefore the Kozeny-Carman equation / theory can not be applied to describe the correlation between filtration time and size distribution.

**Comparison of pulp and filtrate** When comparing the ash content (From table 5.1 on page 22) in the paper resources with the concentration of  $\text{Ca}^{++}$  ( Table 5.5 on page 33) in the pulp there is a clear relation. The higher the content of ash in the paper, the larger the content of  $\text{Ca}^{++}$  in the pulp.

When comparing the ash content in the paper with the ash content in the filtrate the same tendency is present. This is caused by the fact that there is a relationship between  $\text{Ca}_{pulp}^{++}$  and  $\text{Ca}_{filtrate}^{++}$  on approximately 20 % in all cases, except for A1. When the relationship between  $\text{Ca}_{pulp}^{++}$  and  $\text{Ca}_{filtrate}^{++}$  is only 12 % for A1. This could be caused by a better retention in the filter cakes, or the fact that this is only measured on one single filtration in each case, so the 12 % is an outlier.

**Filtrationtime** The mean filtration time was not reproducible, but the order in which the filtration was completed in the three filtrations were the same, as illustrated in figure 5.17. The filtration of A1 was over in 28 sec., 10.8 sec. and 10.6 sec., while A2 took a little longer in all experiments: 35 sec., 15 sec. and 17.4 sec.. The filtration time of the B-series were more similar, the filtration time of B1 was 6 sec., 3.6 sec., and 3 sec., B2 took 5.8 sec., 3.2 sec., and 3 sec. to filtrate, and B3 took 6.2 sec., 3.8 sec. and 4 sec. to

---

dewater.

Eventhough the filtrations could not be reproduced, the tendencies are the same both when considering the order of dewatering times and the specific filter cake resistance. When pulping on only five or six sheets of paper the heterogeneity of the paper will have a larger influence than when examined a larger amount of sample. The results within the same pulp was similar. The pulping time were similar, so the difference between the pulps must come from the paper ressource.

Another effect is the humidity. The ratio between water and paper were only determined once. Therefore there can be a difference in the real drymatter content of the pulps, when comparing to the theoretical.

The theoretical drymatter content of the pulps was 3% (w/w) when pulping and 1% (w/w) when filtrating. When measuring the drymatter content of the pulp, there was only measured once at each pulp. The differences in drymatter content could be caused by heterogeneity of the samples.

The reason for the difference in the pressure curves in the filtrations between the A-series and the B-series can be caused by the faster dewatering (Figures 5.12 and 5.13 on page 28). The consolidation is observed on the pressure curve when the filtration is fast. When the consolidation happens over longer time the pressure it not as affected.

Another explanation can be the higher water content in the filter cakes from the A-series, since the higher the water retention, the poorer the consolidation and therefore the pressure curves show no consolidation.

**Ruth plot and  $\alpha$ -values** The mean  $\alpha$ -values from the first filtrations were determined to be  $1.81 \times 10^{11} \pm 5.12 \times 10^{10} \frac{m}{kg}$ ,  $1.79 \times 10^{11} \pm 4.26 \times 10^{10} \frac{m}{kg}$ ,  $4.38 \times 10^{10} \pm 3.80 \times 10^9 \frac{m}{kg}$ ,  $4.25 \times 10^{10} \pm 5.94 \times 10^9 \frac{m}{kg}$  and  $3.89 \times 10^{10} \pm 1.06 \times 10^{10} \frac{m}{kg}$  for A1, A2, B1, B2 and B3, respectively (Figure 5.19 on page 32). Since the  $\alpha$ -values are determined from the Ruth plots, they should not depend on the pressure, but neither of the  $\alpha$ -values are the same in the repetitions. Eventhough, the tendency is that the A-series has larger  $\alpha$ -values than the B-series in all repetitions.

The large standard deviations can be caused by the bad linearity of the Ruth plots. The  $R^2$ -values are better for the B-series than the A-series, but neither series show a  $R^2$ -value higher than 0.87.

Since the intersections with secondary axis were negative or close to zero and the pressure decreased during the filtrations, it was not possible to determine the  $R_m$ -values. However, in cake filtrations, most of the resistance is from the filter cake, the filtermedium is only present to start the formation of the filter cake.

**Drymatter content of filtercakes in filtrations** The drymatter content of the filter cakes are higher for the B-series than the A-series. While the A-series achieved a drymatter content on  $21.68 \pm 1.48$  % (w/w) for A1 and  $22.17 \pm 0.45$  % (w/w) for A2, the drymatter content in the B-series is  $25.45 \pm 0.32$  % (w/w),  $24.56 \pm 0.32$  % (w/w) and  $26.06 \pm 0.45$  % (w/w) for B1, B2 and B3, respectively. The larger the drymatter content in the filter cakes, the less amount of water retained in the cake and therefore the larger amount of filtrate. This means, that a fast filtration in these experiments is also a good filtration.

The DM contents of the filter cakes in table 5.4 on page 30 shows, that the dewatering of the filter cakes were more effective in the B-series than in the A-series. Therefore, the data show, that longer and wider fibres from the A1-series give longer filtrations with bad dewatering of the filter cakes. This can be explained by the larger distribution of fibre sizes in the A-series, giving a slower dewatering of the filter cakes.

**Strenght characterization of filtercakes** From the tensile stress analysis of A1, the stress-strain curves in figure 5.23 on page 35 show a rapid decrease in stress, after a maximum load has been obtained. According to the theory in section 2.2.3 on page 11 this implies, that the filter cakes of A1 are brittle. Figure 5.24 on page 35 shows the stress-strain curves for B1. These did not show the same rapid decrease in stress as A1. Therefore, the figure shows, that A1 is more brittle than B1. Therefore, the curves for B1 appear more ductile than A1.

Young's modulus from the tensile stress tests of A1 and B1 filter cakes presented in figure 5.25 on page 36 showed no significant difference in strength between the samples. However, the maximum load on the filter cakes showed stronger filter cakes of A1,  $2.26 \times 10^6 \pm 6.76 \times 10^5$  Pa compared to B1,  $9.25 \times 10^5 \pm 3.37 \times 10^5$  Pa. The distribution of data is high with standard deviations corresponding to about 30 % of the mean values. This could be because of inhomogeneity of the filter cakes analyzed. Though, the weight of the bones in table 5.6 on page 34 only had deviations lower than the deviations in the maximum load and E-values, and can thus not explain the high distribution. Instead, the high distributions of maximum load and E-values might be caused by a too low number of repetitions. The E-values calculated from the deformation tests did not show any significant difference in strength of the filter cakes. There was neither any significant difference in maximum load of the filter cakes. The only difference was observed from the strain, as the filter cakes of A1 broke at a higher strain value than B1.

---

**Filtration of the mixed pulp of A1 and B1** It was expected that the mixing would give a filtration time between the filtration times of A1 and B1.

In order to find the best way to use the influence the raw materials has on the pulp's dewatering time and drymatter content of the filter cakes. One thing that was examined were the mixing of two pulps in order to make as even a pulp in size distribution and examine if the tendencies of Chapallah et al (2009) would be observed when mixing pulps. Similar tendencies as Chapallah et al (2009) was observed. Just by adding 10 % (w/w) of another pulp the filtration was improved both timewise, mass of filtrate increased and so did the drymatter content of the filtercake, when compared to the filtrations on 100 % (w/w) B1. As illustrated in figure 5.29 on page 40, 30 % (w/w) A1 and 70 % (w/w) B1 gave the fastest dewatering, highest drymatter content and highest amount of filtrate. In the remaining mixes the dewatering time decreased, but the pulp of 90 % (w/w) A1 and with 10 % (w/w) of B1 had a better dewatering than the 100 % (w/w) A1.

An estimation of the size distribution of the various mixes did not provide the full explanation on why the 30:70 mix had the best dewatering time. The mean length of the various mixes were  $0.99 \pm 0.67$  mm,  $1.08 \pm 0.78$  mm,  $1.17 \pm 0.86$  mm,  $1.26 \pm 0.93$  mm and  $1.35 \pm 0.99$  mm, for 10:90, 30:70, 50:50, 70:30 and 90:10, respectively. Beside the size distribution the packing of the materials has an increasing effect on the dewatering.

**Drymatter content of filtercakes from the filtration on mixed pulps** The same tendency is present for the drymatter content in the filtrations on the mixing experiments (Table 5.10 on page 41 as in the ordinary filtrations. Mentioning the mean drymatter content of the filter cakes in the following order: First 0:100, 10:90, 30:70, 50:50, 70:30, 90:10 and for 100:0:  $22.57 \pm 1.61$  % (w/w),  $24.23 \pm 0.54$  % (w/w),  $24.55 \pm 0.10$  % (w/w),  $23.71 \pm 0.18$  % (w/w),  $22.07 \pm 0.68$  % (w/w),  $21.34 \pm 0.37$  % (w/w) and finally  $20.12 \pm 1.55$  % (w/w). Again it is evident, that a fast filtration is a good filtration.

**Conservation of mass** In table 5.4 on page 30 and table 5.10 on page 41 there is mainly mass conservation when calculating the difference between the added pulp and the remaining filtrate and the wet filter cake. In the variation experiment the difference is  $2.00 \pm 0.66$  % (w/w). In the other filtrations there is a difference of  $1.60 \pm 1.27$  % (w/w) and two of them are negative. Since there can not be more mass than added, the mistake is uncertainties at the mass of filtrate, mass of wet cake or mass of pulp. Since the mass of filtrate is weighed separately at the mixing experiments the values are more valid. There is at maximum 3 % waste of mass in the container, hose or filtration cup.

## 7. Conclusion

Pulps of printing paper show a lower filtration time than pulps of newsprint. The specific filter cake resistances from newsprint are higher than the printing paper pulps, validating the higher filtration time.

The drymatter content in the filter cakes from the printing paper are higher than the ones from newsprint. This shows a better dewatering of the filter cakes and a lower retention of water.

The size distribution are more even in the pulps of printing paper, eventhough the newsprint pulps has the highest mean lengths. Newsprint also has the largest standard deviations in fibre length. This means that the wider distribution of fibre sizes results in a poorer dewatering.

The mixing of newsprint and printing paper pulps show that the mixing improves the dewatering. The most effective dewatering is achieved when filtrating a pulp blend of 30 % (w/w) newsprint and 70 % (w/w) printing paper.

No significant difference between filter cakes from newsprint and filter cakes from printing paper when regarding the strength is observed. There are tendencies that newsprint filter cakes is more brittle than printing paper filter cakes and has a larger max load, but the standard deviations is too large to be conclusive.

# 8. Nomenclature

Table 8.1: Overview of the nomenclature in this Thesis

A	Cross sectional area	
$A_0$	Initial cross sectional area of filter cake	
$A_{pore, surface}$	Surface area of the pores	
$\alpha$	Specific filter cake resistance	
$C_{filtrate}$	Concentration of $Ca^{++}$ in filtrate	
$C_{pulp}$	Concentration of $Ca^{++}$ in pulp	
dP	Difference in hydraulic pressure	
dt	Period of time	
dV	Change in volume	
dz	Thickness of filtermedium	
$D_h$	Hydraulic diameter	
DM cake	Drymatter content in filter cake	
E	Young's modulus	
$\epsilon$	Strain	
$\phi$	Porosity	
h	Height of filter cake	
k	Permeability	
$k_1$	Constant	
$k_2$	Constant	
$k_3$	Constant	
$k_4$	Constant	
$k_5$	Constant	
l	Length of filter cake	
$l_0$	Initial length of filter cake	
$l_{fibre}$	Length of fibre	
$m_{cake,W}$	Mass of wet cake	
$m_{filtrate}$	Mass of filtrate	
$m_{pulp}$	Mass of pulp	
$\mu$	Viscosity	
P	Pressure	
$P_{load}$	Applied load	
$\Delta P$	Difference in pressure	
r	Radius of fibre	
R	Gas constant	$\frac{m^3}{mol \cdot K}$
$R_c$	Cake resistance	
$R_m$	Filter medium resistance	
$R^2$	Coefficient of determination	
s	Concentration of solid in slurry	
$S_o$	Specific surface area	
$\sigma$	Stresses	
T	Temperature	K, °C

Continued on next page

**Table 8.1 – continued from previous page**

$u$	Volume flow rate pr. unit cross-sectional area	
$v$	Velocity	
$v_0$	Velocity in empty tower	
$V$	Volume	
$V_{pores}$	Volume of the pores in filter cake	
$V_{tot}$	Volume of filter cake	
$w$	amount of cake deposited	

# Bibliography

- [Chellappah et al., 2009] Chellappah, K., Tarleton, S., and Wakeman, R. (2009). *Proceeding L-Sessions, vol. 1: Constant pressure filtration of fibre/particle mixtures*.
- [Clement et al., 2004] Clement, K. H., Fangel, P., Jensen, A. D., and Thomsen, K. (2004). *Kemiske enhedsoperation*. Polyteknisk forlag, 5th edition.
- [Condie et al., 1996] Condie, D. J., Hinkel, M., and Veal, C. J. (1996). Modelling the vacuum filtration of fine coal. *Filtration and Separation*, pages 824–834.
- [Dias et al., 2004] Dias, R. P., Teixeira, J. A., Mota, M. G., and Yelshin, A. I. (2004). Particulate binary mixtures: Dependence of packing porosity on particle size ratio. *Industrial Eng. Chem. Res.*, 43(24):7912–7919.
- [Evert, 2006] Evert, R. F. (2006). *Esau's Plant Anatomy Meristems, Cells, and Tissues of the Plant Body - Their Structure, Function, and Development*. Wiley, 3rd edition.
- [Göttsching and Pakarinen, 2000] Göttsching, L. and Pakarinen, H. (2000). *Recycled Fiber and Deinking*. Fapt Oy, 1th edition.
- [Ingmanson, 1952] Ingmanson, W. L. (1952). An investigation of the mechanism of water removal from pulp slurries. *Technical Association of the Pulp and Paper Industry*, 35(10):439–448.
- [Karlsson, 2006] Karlsson, H. (2006). *Fibre Guide Fibre analysis and process application in the pulp and paper industry*. AB Lorentzen and Wettre.
- [Lindau, 2008] Lindau, J. (2008). *Pulp displacement washing An investigation of fibre and bed properties using a novel measurement technique*. Ph.D.-thesis, Chalmers University of Technology.
- [Lundgaard and Nielsen, 2005] Lundgaard, T. and Nielsen, S. B. (2005). *Biologisk indflydelse på kolloidkemi i pulp - Produktion af støbepap hos Brdr. Hartmann A/S*. Afgangsprojekt Aalborg Universitet.
- [Norton, 2006] Norton, R. L. (2006). *Machine design An integrated approach*. Pearson International Edition, 3rd edition.
- [Ramaswamy, 2003] Ramaswamy, S. (2003). Vacuum dewatering during paper manufacturing. *Drying Technology*, 21(4):685–717.
- [Roberts, 1996] Roberts, J. C. (1996). *Paper chemistry*. Blackie Academic & professional, 2. edition.
- [Stougaard and Jensen, 2006] Stougaard, A. and Jensen, K. J. (2006). Undersøgelse af muligheder for styring af papirpulpes afvandingssegenskaber ved målrettet flokkuleringsstrategi og undersøgelse af begrænsninger i afvandingen på grund af creep - med udgangspunkt i produktion af støbepap på brødrene hartmann a/s. Spring semester report.

- [Tao et al., 2003] Tao, D., Parekh, B. K., Liu, J. T., and Chen, S. (2003). An investigation on dewatering kinetics of ultrafine coal. *International Journal of Mineral Processing*, 70:235–249.
- [Wakeman and Tarleton, 1999] Wakeman, R. and Tarleton, E. (1999). *FILTRATION, Equipment Selection Modelling and Process Simulation*. Elsevier Advanced Technology, 1st edition.
- [Walker, 2006] Walker, J. C. F. (2006). *Primary Wood Processing Principles and Practice*. Springer, 2nd edition.



# A. Hartmann Process

The following chapter is written after a conversation with Rasmus Friche, Project Manager at Brødrene Hartmann A/S.

The process at the different plants of Brødrene Hartmann A/S can vary because of local circumstances that makes another option more favorable. Some of the plants uses other additives than the ones described.

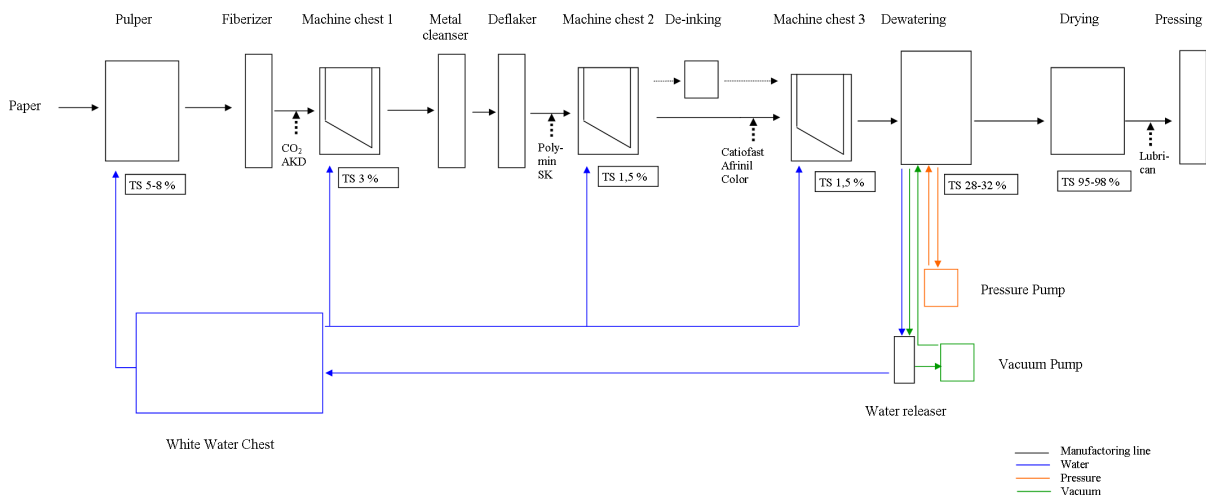


Figure A.1: Processoverview of the moulded fibre process at Hartmann.

## Pulping

The recycled paper (60 % newsprint, 40 % coated paper) is added to the pulper along with water so the dry matter content is 5-8 % approximately. The water is white water from the white water chest, but it is necessary to add approximately 5-6 liter of fresh water pr 1 kg of fibre. The paper is pulped to a homogeneous pulp slurry. The pulp is then passing through a fiberizer, which sort out insoluble matter. CO<sub>2</sub> and AKD-glue is added just before the pulp reaches the 1st machine chest. CO<sub>2</sub> is added to adjust pH to 6.5-7, the aim is 6.8. AKD-glue is added to secure watersizing, water resistance.

## 1st machine chest

The main task is to mix the additives from above with the pulp. More water is added, so the total dry matter content is 3 %. The pulp slurry then passes through a metal cleanser which removes metal parts, such as paper clips, and stones. Afterwards it is passing a deflaker, which ensure the pulp slurry as comminute as possible. Polymin SK is added to start the flocculation. Polymin SK is a short polymer.

---

## 2nd machine chest

Polymix SK is mixed well with the slurry while the dry matter content is changed to 1.5 %. Afterward the pulp has been through machine chest 2 it can either continue to machine chest 3 directly or with a detour to the de-inking system first.

## 3rd machine chest

While the dry matter content is adjusted to 1-1.2 %, Catiofast, Afrinil and if necessary any color is added. Catiofast is an anionic trash catch. Afrinil is added to reduce the formation of foam. After a long mixing period, the pulp is ready to be formed into the relevant moulded fiber form.

## Dewatering

[H]

The form is a positive, slightly larger version than the wanted product build of a metal mesh placed on a drum. The process takes place in several stages. As illustrated in step 1 vacuum is applied on the form which is submerged in the pulp, and the filter cake starts to build up. At first when vacuum is added a lot of fines get sucked through the mesh until there is filter cake enough to stop them. This formation happens while the drum swivels in step 1 and 2. While vacuum is added, water gets sucked up too. In step 3 the form is no longer submerged and the dry-filtration takes place until there is breakthrough of air in step 4. At some plants there is water steam improving the dry-filtration. Then in step 6 air is blown from a compressor to release the moulded-fiber product from the vacuum drum to the drum placing the products on a wire as illustrated in step 7. The dry matter content is now 28-32 %. The water sucked up by the vacuum is afterwards released in the water releaser and is then lead back to the white water chest.

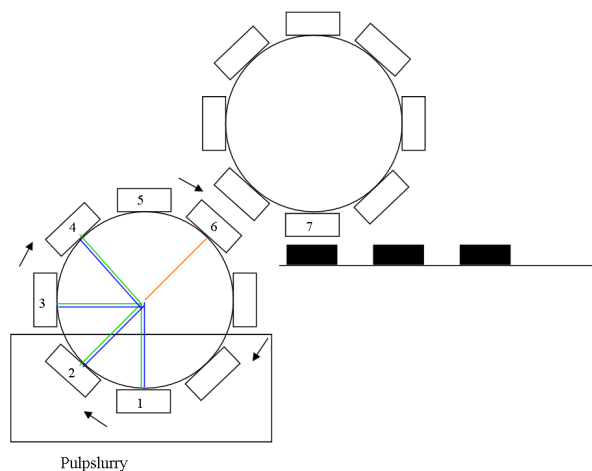


Figure A.2: Overview of the dewatering process.

## Drying

The moulded products are then dried. The drymatter content is afterwards 95-98 %. A lubricant is sprayed on the products so they can be piled up and still easily let go of each other. Before they get piled up, the products are afterpressed to ensure an even surface. In some cases the products get printed on before the pile up too.

## Quality

In order to assure that the products can satisfy the quality standards they are tested for several things such as water resistance, strength, brightness etc. The drymatter content of the papermaterials are examined. It is necessary for the products that the dry-filtration is effective, otherwise the products can not retain their shape. After the products are dried the strength of the products and the watersizing of the products is examined. The piles of products are examined to ensure they can de-nest, i.e. that they can be pulled from each other with out any resistance. There are also aesthetic demands, such as the print has to be centered and distinct. The color of the products has to be uniform.